The behavior of sympatric sea urchin species across an ecosystem state gradient

Dominic Franco C. Belleza[1], Takeshi Urae[1], Shin-ichiro Tanimae[1], Kento Toyama[2], Akari Isoda[2], Gregory N. Nishihara[1,3]

[1]Graduate School of Fisheries and Environmental Sciences, Nagasaki University, Nagasaki city, Nagasaki, Japan
[2]Faculty of Fisheries, Nagasaki University, Nagasaki City, Nagasaki, Japan
[3]Organization for Marine Science and Technology, Institute for East China Sea Research, Nagasaki University, Nagasaki City, Nagasaki, Japan

Corresponding Author:
Dominic Franco C. Belleza[1]
Nagasaki University Institute for East China Sea Research, Taira-machi 1551-7, Nagasaki 851-2213, Japan
Email address: dfcbelleza@gmail.com

Abstract

Background. In temperate macroalgal forests, sea urchins are considered as a keystone species due to their grazing ability. Given their potential to shape benthic communities, we monitored the habitat use by three sympatric sea urchin species and compared their behaviors in a vegetated habitat (VH) and an adjacent isoyake habitat (IH).

Methods. We monitored the environmental conditions and sea urchin density along deep and shallow transects of the VH and IH for over a year. The benthic rugosity at both sites were also surveyed. A mark-recapture experiment was conducted on the two most abundant sea urchins, *Diadema setosum* and *Heliocidaris crassispina*, to elucidate sea urchin movement patterns and group dynamics.

Results. We found that exposure to waves was highest at the VH while the IH was sheltered. The deep IH experienced the least amount of light due to high turbidity. Water temperature patterns were similar across sites. The VH benthic topography was more rugose compared to the smoother and silt-covered IH substate. Peak macroalgal bloom occurred three months earlier in IH, but macroalgae persisted longer at the shallow VH.

Among the sympatric sea urchins, *H. crassispina* was most abundant at the shallow VH and was observed in pits and crevices. The most abundant across IH and in the deep VH was *D. setosum,* preferring either crevices or free-living, depending on hydrodynamic conditions. The least abundant species was *Diadema savignyi,* and most often observed in crevices.

40 Small and medium sea urchins were most often observed at the IH, whereas larger sea urchins
41 were more likely observed at the VH.
42
43 The mark-recapture study showed that *D. setosum* was found to displace further at the IH, and *H.*
44 *crassispina* was more sedentary. Additionally, *D. setosum* was always observed in groups,
45 whereas *H. crassispina* was always solitary.
46
47 **Discussion.** The behaviors of sympatric sea urchins, *Diadema savignyi, D. setosum* and *H.*
48 *crassispina,* differed in response to changes in the benthic environment and physical conditions.
49 Sea urchin displacement increased when rugosity and wave action were low. Habitat preference
50 shifted to crevices in seasons with high wave action. In general, the mark-recapture experiment
51 showed that sea urchins displaced further at night.
52

53 **Introduction**
54 The resilience of natural ecosystems is limited and highly dependent on many factors including
55 effect size, persistence, and the synergistic effects of multiple disturbances (*Nyström, Folke &*
56 *Moberg, 2000*; *Benedetti-Cecchi et al., 2001*; *Strain et al., 2014*). A unique characteristic of an
57 ecosystem is the ability to switch among a variety of alternative states (*Scheffer et al., 1993*,
58 *2001*; *Carpenter, Ludwig & Brock, 1999*; *Xu et al., 2015*). Some examples are coral-macroalgal
59 phase shifts (*McManus & Polsenberg, 2004*), shift from clear to turbid phase in lakes (*Scheffer*
60 *et al., 1993*), and forest-open landscape phase shifts (*Xu et al., 2015*). Macroalgae ecosystems are
61 no exception, because subtidal vegetated ecosystems can collapse into a state where the rocky
62 substrate is bare of macrophytes and habitat complexity and primary productivity are low
63 (*Filbee-Dexter & Scheibling, 2014*; *Krumhansl et al., 2016*; *Pessarrodona et al., 2021*). Such
64 phase shifts (i.e., degradation of macroalgal forests) can be caused by both abiotic (*Seymour et*
65 *al., 1989*; *Airoldi, 1998*; *Coleman et al., 2008*; *Provost et al., 2017*) and biotic disturbance
66 (*Yamaguchi et al., 2010*; *Poore et al., 2012*; *Vergés et al., 2016*), and these events have been
67 documented for more than 100 years in Japan, where algae bed degradation is known as *isoyake*
68 (*Fujita, 2010*).
69
70 Isoyake is a Japanese concept of seaweed deforestation caused by a combination of fluctuating
71 oceanographic conditions and increasing herbivory (*Graham, 2010*). Compared to sea urchin
72 barrens where sea urchin overgrazing is the main cause, the term isoyake is used to describe the
73 degraded state of a temperate algal bed where the cause is less clearly defined and implies that
74 some phenomenon has caused the deforestation or degradation of algal forests (*Graham, 2010*;
75 *Eger et al., 2022*; *Sato et al., 2022*). In particular, the life cycle of canopy-forming seaweeds in
76 Japan have experienced a marked decrease in growth and biomass in summer, associated with
77 warm surface temperatures and low nutrient supply (*Haroun, Yokohama & Aruga, 1989*;
78 *Serisawa et al., 2004*). Unfortunately, oceanographic studies in the East China Sea region show
79 steadily increasing sea surface temperatures of about 0.3°C year^{-1} and stratification of the water-
80 column (*Son et al., 2012*; *Lee & Kim, 2013*). The rapidly changing environment has created

81   unsuitable conditions for economically important seaweeds to thrive while conventional seaweed
82   production is now more sensitive to climatic and human disturbances (*Chen, 2019*).
83

84   Sea urchins are highly successful benthic grazers because their natural population control is
85   limited to a few specialized predators (*Estes & Palmisano, 1974*; *Fujita et al., 2013*; *Kawamata*
86   *et al., 2016*). Although they are often considered herbivores, sea urchins have flexible dietary
87   requirements that enable them to switch to omnivory (*Agnetta et al., 2013*; *Rodríguez-Barreras*
88   *et al., 2015*; *Leclerc et al., 2021*) and cannibalism at higher densities (*LeGault & Hunt, 2016*) or
89   in rare cases, even directly attack their predators (*Clements, Dupont & Jutfelt, 2021*). This
90   dietary flexibility enables sea urchins to exploit and overwhelm primary producers in rocky reefs
91   and cause a phase shift (*Tuya, Martin & Luque, 2004*; *Lauzon-Guay, Scheibling & Barbeau,*
92   *2009*; *Flukes, Johnson & Ling, 2012*), while maintaining the barren state by subsisting on a
93   mixed diet of small algae and benthic invertebrates (*Bonaviri et al., 2011*). In pristine algae bed
94   ecosystems, sea urchin populations are controlled by predation (*Tegner & Levin, 1983*; *McKay &*
95   *Heck, 2008*; *Gregr et al., 2020*). Here, the abundant supply of drift algae provides sea urchins
96   with a reliable food source and they are less likely to forage on the standing algal biomass
97   (*Kriegisch et al., 2019*).
98

99   Sea urchins avoid direct competition with other sea urchin species through omnivory and
100   resource partitioning (*Contreras & Castilla, 1987*; *McClanahan, 1988*; *Vanderklift, Kendrick &*
101   *Smit, 2006*). Stable isotope analysis suggests that sympatric sea urchin species occupy different
102   trophic levels (i.e., herbivory vs. omnivory) despite habitat overlap (*Vanderklift, Kendrick &*
103   *Smit, 2006*). For example, specialized structures such as modified aboral podia in *Loxechinus*
104   *albus* allows the capture of floating algal pieces while *Tetrapygus niger* specializes in the
105   efficient consumption of benthic algae due to its longer pyramid structures in the Aristotle's
106   lantern (*Contreras & Castilla, 1987*). Benthic communities, depth and temperature can vary
107   widely across latitudes (*Guidetti & Dulčić, 2007*; *Williams, Coleman & Jordan, 2020*). This
108   results in large (*Leclerc et al., 2021*) or few variations (*Vanderklift & Wernberg, 2010*) in the
109   diet and feeding behavior of conspecific urchins. Nevertheless, this makes sea urchins highly
110   adaptable to their environment and a particular species may display different behavioral patterns
111   when in an algal bed or when in a barren (*Yusa & Yamamoto, 1994*; *Urriago Suarez et al., 2021*).
112   However, there is little evidence of simultaneous comparison between both states in field
113   conditions because contrasting states from the same ecosystem are often separated by several
114   decades (*Krumhansl et al., 2016*).
115

116   Our study explores the benthic community of a small embayment where two ecosystem states are
117   temporally co-occurring at a relatively small spatial scale (i.e., 100's of m). We monitored the
118   abundance and distribution of three sympatric sea urchin species, *Diadema savignyi*, *Diadema*
119   *setosum* and *Heliocidaris crassispina*, along a vegetated and an isoyake area for over a year
120   (September 2020 – December 2021) and also analyzed the movement patterns of the two most

121 abundant sympatric sea urchin species, *D. setosum* and *H. crassispina* through a mark-recapture
122 experiment. Morphologically, Diadematid sea urchins (i.e., *D. savignyi*, *D. setosum*) differ
123 greatly from *H., crassispina*. Adult Diadematid sea urchins have larger test sizes (6 – 9 cm)
124 compared to adult *H. crassispina* (5.5 – 7 cm), and also have long and thin venomous spines up
125 to 20 cm, while *H. crassispina* have short and hard, but non-venomous spines (3 – 5 cm).
126 Whereas *H. crassispina* has a dark purple color, both Diadematid species are black, with *D.*
127 *savignyi* having distinct bright blue lines along the ambulacral zones while *D. setosum* have five
128 white spots on the aboral side, one each along the ambulacral zone. Diadematid urchins are
129 known to form aggregations (*Pearse and Arch, 1969*) while *H. crassispina* are solitary (*Yusa and*
130 *Yamamoto, 1994*). Because of the differences between species, we hypothesized that the
131 substrate component and environmental conditions affect sea urchin behavior and movement
132 patterns while sea urchin species and size determine microhabitat preference.
133
134 **Materials and Methods**
135 **Study Site**
136 The study was conducted at Arikawa Bay (Fig. 1), located in northeastern Nakadori Island of the
137 Goto Islands, Nagasaki Prefecture, Japan (129.11°E, 32.99°N). The study site presents a case of
138 contrasting ecosystem states where a vegetated and an isoyake habitat are spatially adjacent but
139 physically separated by a concrete structure (Fig. 1, inset).
140
141 Arikawa Bay is exposed to wind and waves from the north. In general, the coastline is rocky
142 while some parts are armored with concrete walls and wave-breakers. We examined two distinct
143 ecosystems: (A) a vegetated habitat, hereafter known as VH and (B) an isoyake habitat, hereafter
144 known as IH. Within each ecosystem, a 20-meter stretch of rocky reef was selected for
145 monitoring in deep (4.27±0.60 m mean±SD at IH and 4.62±0.62 m at VH) and shallow areas
146 (2.07±0.60 m at IH and 3.06±0.67 m at VH).
147
148 The VH is open to the north (i.e., windward side of a concrete jetty) and has a mean wind fetch
149 of 2342 m (number of vectors reaching maximum limit: 13) (*Sato et al., 2022*) (see Fig. S1,
150 Supplementary figures). The substrate is mostly consolidated rocks and small to medium-sized
151 boulders. The VH is dominated by small algae (*Corallina* spp., *Gelidium* spp.) and turf algae
152 present year round and sparse patches of perennial *Sargassum macrocarpum*. Blooms of
153 seasonal macroalgae (i.e., *Sargassum horneri*, *Asparagopsis taxiformis*, *Dictyopteris* spp.,
154 *Codium fragile, Colpomenia sinuosa* and *Hydroclathrus clathratus*) occur in mid to late spring
155 and persist until early to mid-summer. The IH is located behind a concrete jetty and is sheltered
156 from waves approaching from the north (Fig. 1, see inset) and has a mean wind fetch of 1889 m
157 (12). The IH substrate is also rocky, however silty patches occur in the deeper areas. The rocky
158 surfaces are bare, except for a few patches of encrusting coralline algae apart from the seasonal
159 macroalgal bloom (i.e., *S. horneri, C. sinuosa, H. clathratus*) that occurs from spring to early
160 summer.

161
162 **Field monitoring**
163 To determine changes in the benthic environment, we conducted monitoring activities by skin
164 diving in the daytime (ca. 07:00 – 08:00), along marked sections in the deep and shallow reefs of
165 VH and IH. A 20-meter rope was secured to the substrate on both ends and set parallel to shore
166 to guide the installation of a transect tape every monitoring period. Photos of the substrate were
167 taken using a 1 m tall, 1 m² polyvinyl chloride (PVC) photoquadrat (*Preskitt, Vroom & Smith,*
168 *2004*) with a GoPro Hero 8 camera at 1 m intervals along each belt transect. A total of 10 photos
169 were taken for each belt transect every monitoring activity. For the sea urchin monitoring, all sea
170 urchins observed within a 2-meter-wide swath at 1 m intervals (2 × 1 m) along the transect
171 were recorded for their species and whether they occupied pits, crevices, or were free-living
172 (*Yusa & Yamamoto, 1994*; *Gravem & Adams, 2012*; *Frey & Gagnon, 2016*). A total of 10, 2 ×
173 1 m swaths were examined for each belt transect every survey period and the body diameter of
174 all sea urchin species found were measured using a caliper *in situ*. Sea urchin sizes were
175 classified as small (< 3.9 cm), medium (4.0-5.9 cm) or large (> 6 cm). Five sea urchin species
176 occur at the study site, which include *Hemicentrotus pulcherrimus*, *Toxopnuestes pileolus*, *D.*
177 *savignyi*, *D. setosum*, and *H. crassispina*. Of these, *H. pulcherrimus* was cryptic, usually found
178 under boulders and was observed along the transect only once, whereas *T. pileolus* were
179 scattered widely, and only thirteen individuals were found during the monitoring period. Given
180 the scarcity of *T. pileolus* and *H. pulcherrimus*, they were not included in the formal analysis.
181 Sea urchin biomass was estimated from sea urchin size-weight relationship determined by fitting
182 a generalized linear model (GLM) on the weight and size from 10 randomly collected individuals
183 of *D. savignyi*, *D. setosum* and *H. crassispina* from the shallow and deep transects.
184
185 Quadrat photos were downloaded from the camera and 50 points were randomly plotted on each
186 photo across a 10 × 10 grid via R (*R Core Team, 2022*) using the magick (*Ooms, 2021*) and
187 imager (*Barthelme et al., 2021*) packages. Each point was identified and classified whether they
188 were macroalgae, coralline algae (i.e., encrusting, geniculate), turf algae, substrate (i.e., rock,
189 sand, silt), or other (i.e., debris, benthic animals). Benthic elements not associated with benthic
190 cover (i.e., other) were excluded from the analysis.
191
192 Environmental conditions were recorded using data loggers. For each habitat, one wave height
193 logger (Infinity-WH AWH-USB, Alec Electronics Co., Japan) was deployed at a point midway
194 between the deep and shallow transects. For each deep and shallow belt transect, one depth
195 logger (HOBO U20, Onset Computer Corp., Bourne, Massachusetts, USA) and one
196 temperature/ light logger (HOBO Pendant MX2202, Onset Computer Corp., Bourne,
197 Massachusetts, USA) was installed. The instruments recorded environmental data at 10-minute
198 intervals for 20 – 25 days each month before retrieval and data offloading. The monthly daily
199 averages for wave height (m) and temperature (ºC) were calculated for each month. The monthly

200 average of the integrated photosynthetic photon flux density (PPFD, mol m^{-2} day^{-1}) was also
201 calculated for each month.
202
203 **Sea urchin mark-recapture experiment**
204 To measure sea urchin movement patterns within a 24 h period, mark-recapture experiments
205 were conducted in late August to early September 2020 on the two most abundant sea urchin
206 species at the study sites; the long-spined black sea urchin, *D. setosum* and the purple sea urchin,
207 *H. crassispina*. Whereas *D. setosum* occurred in groups of 2 – 30 individuals, *H. crassispina* was
208 solitary. Twenty individuals each of *D. setosum* and *H. crassispina* from each habitat were
209 selected, while ensuring that the individuals were separated by at least 5 m. The initial location
210 of all individuals was marked by placing numbered buoys. A numbered plastic T-bar tag was
211 inserted into the inter-ambulacral region using a tagging gun with a 0.5 mm diameter needle
212 (*Rodríguez-Barreras & Sabat, 2015*), and each tagged individual was treated as one trial. All
213 tagged sea urchins were returned to their original position and the number of individuals which
214 composed the group at the initial location, were also recorded. The initial capture and tagging
215 activity was conducted between 06:00 to 07:00, labelled as "start" and assigned a linear distance
216 of 0 m. The first recapture occurred after 12 h (i.e, 18:00) and the second recapture was after
217 another 12 h (i.e., 6:00 – 7:00 on the next day). About 5 – 10 min was allocated for recapturing
218 the tagged sea urchins via a circular search pattern by snorkeling. Once a tagged individual was
219 found, the marked buoy was moved to the new location and the linear displacement was
220 measured. Those not found during the recapture were labelled as lost and excluded from the
221 analysis.
222
223 **Benthic rugosity measurements**
224 Rugosity can be used as a proxy to describe substrate complexity, where a flat surface would
225 have a value of one and higher values can describe a more complex benthic structure. Benthic
226 rugosity was measured by laying a 5 m length of stainless-steel chain with 1 cm links along the
227 contour of the rocky reef. A transect tape was laid beside the chain to measure the straight-line
228 length the chain end-points (*Risk, 1972*; *Trebilco et al., 2015*). The straight-line chain length (5
229 m) was divided by the overlaid length of the chain to estimate rugosity. A total of 35 and 25
230 measurements were done at the deep and shallow areas, respectively in the IH and 24 and 36
231 were done at the deep and shallow areas, respectively of the VH.
232
233 **Data analysis**
234
235 **Environmental data and phenology**
236 Poor weather conditions and instrument error with the temperature/ light loggers led to several
237 months with missing data (Supplementary figures, Fig. S2). For example, in the VH, from July –
238 December 2021 (i.e., missing data in the shallow VH from July to December and missing data in
239 the deep VH from July, November, and December), and in January and April 2021, in both sites.

240   The missing temperature and light data were imputed by fitting a generalized additive model
241   (GAM) (Eq. 1) to the datasets. The monthly daily averaged wave heights were determined
242   assuming a gamma distribution with a log link-function, whereas the monthly daily averaged
243   light and temperature data sets were determined assuming a gaussian distribution with a log and
244   identity link-function, respectively. Due to excess zeroes in observations, the sea urchin density
245   dataset was analyzed assuming a hurdle negative binomial distribution with a log link-function,
246   whereas the sea urchin biomass dataset was analyzed assuming a hurdle gamma distribution with
247   a log link-function. For the percent benthic cover, benthic elements were modelled separately
248   due to different patterns in spatial distribution. Due to excess zeroes, coralline, macroalgae and
249   turf elements were analyzed assuming a zero-inflated beta distribution with a logit link-function,
250   whereas the substrate element was analyzed assuming a zero-one inflated beta distribution with a
251   logit link-function. The smoothing function for all GAMs was a cubic regression spline.

252   (1)

$$\mu = g(y,\theta)$$
$$y = f\big(s(x) + \beta_1 + \beta_2\big)$$

$$\beta \sim Normal(0,0.5)$$
$$\theta \sim Student_3(0,1)$$

259   Here, g is the distribution, f is the link-function, s is a smoothing function for time x, μ is the
260   location and θ is the scale of the g, and β is the coefficient for the covariates (i.e., habitat and
261   transect). For the average daily wave height dataset, the predictor variables were the time and
262   location (2 factor levels: IH, VH). For the average daily light and temperature, percent benthic
263   cover, sea urchin density, and biomass datasets the predictor variables were the time, location (2
264   factor levels: IH, VH), and transect (2 factor levels: deep, shallow). For all model priors, the β
265   coefficients were assigned a normal prior with a location of 0 and a scale of 0.5 while θ were
266   assigned Student's t prior with 3 degrees-of-freedom, a location of 0, and scale of 1.

267

268   **Benthic rugosity**
269   The difference in benthic rugosity between IH and VH was analyzed using a generalized linear
270   model (GLM) assuming a Gamma distribution ($\Gamma(\ )$) with a log link-function (Eq. 2). The
271   response variable was the benthic rugosity and the predictor variables were the habitat (2 factor
272   levels: IH, VH) and transect (2 factor levels: deep, shallow).

273   (2)

$$y = \Gamma(\mu,\theta)$$
$$\mu = exp(\alpha + \beta x)$$

$$\beta \sim Normal(0,0.5)$$
$$\theta \sim Student_3(0,1)$$

279

280   Here, the y is the measured benthic rugosity across the deep and shallow transects of the IH and
281   VH; α and β are the model coefficients; x is the predictor variable. The parameters μ and θ are
282   the location and scale of the Gamma distribution. For the model prior, the β coefficients were
283   assigned a normal prior with a location of 0 and a scale of 0.5 while θ was assigned a Student's t
284   prior with 3 degrees-of-freedom, a location of 0, and scale of 1.
285
286   **Sea urchin size-class and microhabitat preference**
287   The size-class and preferred microhabitat of *D. savignyi*, *D. setosum* and *H. crassispina* was
288   analyzed using a GAM assuming a beta distribution with a logit link-function to elucidate the
289   relationship between the proportion of sea urchin species (y) occurring in a particular
290   microhabitat in the IH and VH, and their corresponding size-class during the monitoring period.
291   The model is similar to eq. 1 and the smoothing function for the GAM was a cubic regression
292   spline.
293
294   The predictor variables were habitat (2 factor levels: IH, VH), transect (2 factor levels: deep,
295   shallow), species (3 factor levels: *D. savigny*, *D. setosum*, *H. crassispina*), microhabitat (3 factor
296   levels: pit, crevice, free-living), size-class (3 factor levels: small, medium, large). The β
297   coefficients were assigned a normal prior with a location of 0 and a scale of 0.5 while θ were
298   assigned a Student's t prior with 3 degrees-of-freedom, a location of 0, and scale of 1.
299
300   **Sea urchin movement patterns**
301   The linear displacement by *D. setosum* and *H. crassispina* over a 24 h period during the mark-
302   recapture experiment was analyzed using a GLM, assuming a hurdle-gamma distribution (Lewin
303   et al., 2010) with a log link-function (Eq. 3).
304   (3)

$$y = (1 - \pi)\Gamma(0,\theta) + \pi\Gamma(\mu,\theta)$$
$$\mu = x\beta$$
$$log\frac{\pi}{1 - \pi} = x\alpha$$

$$\beta \sim Normal(0,1)$$
$$\theta \sim Student_3(0,1)$$
$$\theta_{\theta,trial} \sim Student_3(0,2)$$

313   Here, y is the sea urchin displacement over the mark-recapture period; π is the probability of a
314   non-zero value; α and β are the model coefficients; x is the predictor variable. The parameters μ
315   and θ are the location and scale of the Gamma distribution, respectively. The predictor variables
316   were urchin species (2 factor levels: *D. setosum* and *H. crassispina*), habitat (2 factor levels: IH,
317   VH), recapture period (2 factor levels: first recapture, and second recapture), and the
318   experimental trial was treated as a random intercept. The β coefficients were assigned a normal

319   prior with a location of 0 and a scale of 0.5 while θ was assigned a Student's t prior with 3
320   degrees-of-freedom, a location of 0, and scale of 2.
321
322   The change in sea urchin group size was analyzed using a Bayesian GLM which assumed a
323   negative binomial distribution with a log-link function (Eq. 4). For this analysis, *H. crassispina*
324   was excluded since it was solitary throughout the mark-recapture period.
325   (4)

$$y = NegBin(\mu,\theta)$$
$$\mu = exp\left(\beta_1 + \beta_2\right)$$

$$\beta_1 \sim Student_3\left(0, \theta_{\beta_1}\right)$$
$$\beta_2 \sim Student_3\left(0, \theta_{\beta_2}\right)$$
$$\theta \sim Student_3\left(0, \theta_\theta\right)$$
$$\theta_{\beta_{1,trial}} \sim Student_3(0,2)$$
$$\theta_{\beta_{2,trial}} \sim Student_3(0,2)$$
$$\theta_{\theta,trial} \sim Student_3(0,2)$$

326
327
328
329
330
331
332
333
334
335
336   Where, y is the number of *D. setosum* individuals together with the tagged sea urchin during the
337   start, first recapture, or second recapture period; The parameters μ and θ are the location and
338   scale of the negative binomial distribution. The θ and β coefficients were assigned Student's t
339   priors with 3 degrees-of-freedom, a location of 0 and a scale of 2. The predictor variables were
340   the recapture period (3 factor levels: start, first recapture, second recapture), and habitat (2 factor
341   levels: IH, VH), while the period and habitat were nested in the varying intercept, experimental
342   trial.
343
344   All analyses were conducted in R version 4.1.2 (*R Core Team, 2022*). Bayesian methods were
345   used for all models through the brms package (*Bürkner, 2017, 2018*) and assigned weakly
346   informative priors (*Gelman, Simpson & Betancourt, 2017*), where each model was ran with four
347   Markov chains with 4000 iterations per chain. The chains and posterior distributions were
348   assessed visually for convergence (see model validations in Supplementary figures, Fig. S3 –
349   Fig. S17). All models were compared with a similar model having the same distributional
350   parameters but with no explanatory variables (null model) using the difference in the expected
351   log pointwise predictive density (ELPD) of the leave-one-out cross validation (LOO) (Table 1)
352   (*Vehtari, Gelman & Gabry, 2017*). As the data were not normally distributed, we reported the
353   conditional means that were estimated by the Bayesian models.
354

355   **Results**
356   The monthly daily averaged wave heights in the IH and VH over the study period ranged from
357   0.01 to 0.02 m and 0.03 to 0.09 m, respectively (Table S1). The highest waves were recorded
358   from autumn until spring, and it was during this time (July – December 2021) when the

359 temperature/ light loggers were damaged in the shallow VH resulting in missing data. The lowest
360 wave heights were during the late-spring and summer months (Fig. 2A). The light levels in the
361 IH and VH had monthly daily average photosynthetic photon flux densities (PPFD) ranges of
362 1.47 to 16.27 mol m^{-2} day^{-1} and 1.82 to 12.86 mol m^{-2} day^{-1}, respectively (Fig. 2B, Table S2).
363 Meanwhile, the monthly daily average temperature at IH and VH during the study period ranged
364 from 13.24 to 27.05°C and 13.51 to 27.19°C, respectively (Fig. 2C, Table S3). The difference in
365 the expected log point-wise predictive density (ELPD) of the leave-one-out cross validation
366 (Table 1) indicates support for the generalized additive models (GAM) applied to the
367 environmental data over their equivalent null models (*Vehtari, Gelman & Gabry, 2017*).
368
369 The substrate at the VH is composed of rocks and large boulders while the IH benthic
370 composition was mainly small flat rocks and silt. The rugosity GLM shows lower mean
371 rugosities for the deep (1.16) and shallow (1.23) areas for IH, compared to the deep (1.38) and
372 shallow (1.37) areas of VH (Fig. 3, Table S4). Both habitats experienced macroalgal blooms
373 from late winter until early autumn (Fig. 4A, Table S5). In general, peak macroalgal blooms
374 occurred in February for both the deep (11.62%) and shallow (31.10%) IH while peak
375 macroalgal blooms occurred in April (13.44%) for the deep VH and in May (33.36%) for the
376 shallow VH (Fig. 5). The macroalgae composing the blooms in the IH are mostly brown
377 seaweeds (i.e., *Colpomenia sinuosa, Hydroclathrus clathratus* and *Sargassum horneri*) whereas
378 algae in the VH is composed of green (i.e., *Codium* spp.), brown (i.e., *C. sinuosa, H. clathratus,*
379 *Dictyota* spp., *Dictyopteris* spp., *Padina* spp., *Sargassum* spp.) and red algae (i.e., *Asparagopsis*
380 *taxiformis, Martensia jejuensis*). Although the persistence of macroalgal cover (> 1%) at the
381 shallow VH (3.52%) and deep IH (1.10%) occurred until September while the macroalgae at
382 deep VH (2.78%) and shallow IH (1.82%) lasted until August. The relative importance of habitat
383 type and transect depth shows that the macroalgal state was similar in both habitats (Table S6).
384 Outside the macroalgal bloom season, the IH was mostly bare substrate (i.e., rocks and silt), and
385 the substrate cover state persisted throughout the study period (IH deep: 0.446, IH shallow:
386 0.258, Table S6). The substrate cover state also persisted in the deep VH (0.242), while the
387 shallow VH had a lower overall rate of exposed substrate (0.054).
388
389 Among the three sea urchin species, *D. setosum* had similar patterns of densities across all depths
390 in both study sites (Table S6), while *H. crassispina* had an affinity for the shallow VH and IH,
391 followed by the deep VH and deep IH. For *D. savignyi*, its distribution pattern was less clear but
392 its preference for the shallow VH was higher compared to the deep IH. Population-wise, sea
393 urchin densities (Fig. 4B, Table S7) indicated that *D. setosum* was the most common in the deep
394 (1.48 indiv. m^{-2}) and shallow areas (1.32 indiv. m^{-2}) of IH and in the deep VH (2.95 indiv. m^{-2}).
395 In the shallow VH, *H. crassispina* was most common (3.02 indiv. m^{-2}). The least abundant
396 species in all sites was *D. savignyi* (< 1 indiv. m^{-2}). The sea urchin biomass (Fig. 4C, Table S8)
397 in the IH was generally low. In the deep IH, *H. crassispina* had the lowest biomass among the 3
398 species (1.27 – 1.63 g m^{-2}), followed by *D. savignyi* (2.68 – 3.85 g m^{-2}) and *D. setosum* (3.42 –

399   4.52 g m^{-2}), while In the shallow IH, the three species had similar biomass. In the shallow VH,
400   *D. savignyi* had the highest biomass (4.84 – 7.17 g m^{-2}), followed by *D. setosum* (3.40 – 4.50 g
401   m^{-2}) and *H. crassispina* with the least (1.50 – 1.79 g m^{-2}).
402
403   **Sea urchin size-class and microhabitat preference**
404   The sea urchins were distributed widely across the two study sites and had distinct microhabitat
405   preferences during the study period (Fig. 6, Table S9). At the IH, greater than 50% of medium-
406   sized *D. setosum* occurred as free-living during the autumn and early winter months of 2020 and
407   during the summer-autumn months of 2021 (Fig. 6A, B). However, the preference for crevices
408   among *D. setosum* increased from the winter months of 2020 until mid-spring of 2021. The same
409   patterns were observed for the deep and shallow transects of IH. For *D. savignyi*, few sea urchins
410   were recorded at IH. In the deep area, an increasing trend was found for small individuals
411   preferring crevices from spring until summer 2021, while less than 50% were free-living. In the
412   shallow IH, the occurrence of *D. savignyi* in crevices and as free-living was below 25%. For *H.*
413   *crassispina*, sea urchins preferred mostly crevices in the deep IH. Free-living *H. crassispina* in
414   the deep IH occurred only in September of 2020 and 2021 (13.94 and 10.86%, respectively). The
415   *H. crassispina* found in the shallow IH was found in all microhabitat types and almost
416   exclusively composed of medium-sized individuals. However, free-living individuals were not
417   recorded from August to December 2021.
418
419   In the deep VH, *D. setosum* was most abundant (Fig. 6C), composed mainly of small and large-
420   sized individuals and followed similar seasonal patterns of microhabitat preference as those in
421   IH. In the shallow VH, all size classes of *D. setosum* mostly preferred crevices while few
422   medium and large-sized individuals were free-living from spring to late summer of 2021. For *D.*
423   *savignyi*, small and large individuals preferred crevices while small individuals were free-living
424   in the deep VH. In the shallow VH, medium and large individuals preferred crevices while large
425   individuals were free-living. For *H. crassispina*, small sea urchins mostly preferred crevices
426   together with a few large individuals in the deep VH throughout the study period. Although free-
427   living individuals were found in the spring of 2021, *H. crassispina* in the shallow VH generally
428   preferred either pits or crevices throughout the study period.
429
430   **Sea urchin movement patterns**
431   There was a difference between the movement patterns of *H. crassispina* and *D. setosum* across
432   the IH and VH (Fig 7A), with a clear pattern that shows increasing linear distance after the
433   second recapture compared to the first recapture. On average, both species displaced further in
434   the IH than at the VH in the second recapture (Table S10).
435
436   Both species also had distinct social behaviors because *H. crassispina* was always solitary in its
437   crevice or burrow and was not found together with other conspecifics when it was outside. In
438   contrast, *D. setosum* was always observed in groups. The mark-recapture experiment shows that

439   *D. setosum* group composition varied widely in the VH compared to the IH (Fig. 7B). The
440   group-size GLM (Table S11) shows that there was a decrease in the average number of
441   individuals in the first recapture in both IH (from 4.38 to 2.16 indiv.) and VH (from 7.73 to 5.55
442   indiv.) while an increase was observed for the group size in IH (from 2.16 to 5.29 indiv.) but not
443   for VH (from 5.55 to 4.80 indiv.), after the second recapture.
444
445   The relatively large displacement and the changing group size by *D. setosum* caused difficulty in
446   locating the tagged individuals during the recapture periods leading to losses (Table 2).
447   Following the second recapture in VH, 25% (n = 5 indiv.) of tagged *D. setosum* were lost. At IH,
448   30% (n = 6 indiv.) were lost during the first recapture and 50% (n = 10 indiv.) were subsequently
449   lost after the second recapture period. For *H. crassispina*, eighteen individuals in VH remained
450   in their initial positions throughout the experiment while 2 were lost after the second recapture
451   period. All *H. crassispina* were located in the IH.
452

453   **Discussion**
454   For over a year we compared adjacent habitats with contrasting ecosystem states and evaluated
455   how their environmental conditions and benthic phenology varied and how different sympatric
456   sea urchins behaved across both sites. Both sites differed in hydrodynamic conditions as the VH
457   is more exposed while the IH is generally sheltered (Fig. 2A), despite having similar wind fetch
458   patterns (Fig. S1, Supplementary figures). This has large implications for water visibility and
459   sedimentation rates because the deeper parts of IH is generally turbid leading to greater light
460   attenuation (Fig. 2B), possibly affecting benthic communities (Fig. 4A). Although we did not
461   measure productivity, it is known that a stable water column facilitate phytoplankton blooms
462   (*Matsumoto et al., 2021*), especially in bays and sheltered areas. Alternatively, vertical mixing
463   due to tidal fluctuations can also resuspend sediments and lead to turbidity (*Wang, 2002*).
464
465   The macroalgal bloom occurring in spring until summer across both sites is a period of high
466   primary productivity and algal food availability for benthic communities. Interestingly, the deep
467   and shallow IH reached peak macroalgal cover three months earlier compared to the shallow VH
468   but also ended earlier while macroalgal cover persisted until early autumn in the shallow VH.
469   For both habitats, it appears that the benthic macroalgal bloom may be controlled by seasonal
470   environmental cues attributed to changes in environmental variables such as temperature and
471   light (*Yoshida, Yoshikawa & Terawaki, 2001*; *Toste et al., 2003*; *Martínez, Pato & Rico, 2012*;
472   *Gauna, Cáceres & Parodi, 2013*). For example, daylength caused an increase in the growth of
473   the frond length, biomass, branching rate for *Dictyota dichotoma* (*Gauna, Cáceres & Parodi,*
474   *2013*), a species common in the VH but not in the IH. However, we suspect that the
475   asynchronous peak benthic cover and composition of the macroalgal blooms may be due to
476   factors such as nutrient supply. Specifically, the IH is in a semi-enclosed area prone to the effects
477   of terrestrial run-off. Benthic communities close to the source of land-based pollution are known
478   to have lesser diversity and composed of species with simpler thalli forms with relatively short

479 life histories (*Littler & Murray, 1975*) that benefit from rapid uptake of the excess dissolved
480 inorganic nutrients. This may help explain why the macroalgal bloom in the IH is predominantly
481 composed of *Colpomenia sinuosa* and *Hydroclathrus clathratus*. Furthermore, the substrate type
482 may also influence the persistence of benthic algae because hard substrates are better at
483 supporting a high diversity of macroalgae and associated fauna while soft substrates support
484 benthic microalgal communities and burrowing invertebrates (*Chenelot, Jewett & Hoberg, 2011*)
485 and do not provide a stable attachment for seaweed holdfasts. In general, the shallow VH has a
486 wider variety of primary producers composed of seasonal macroalgae and perennial coralline and
487 turf algae, while the entire IH and the deep VH only has a seasonal macroalgal bloom and some
488 coralline algae, while the substrate is generally bare.
489
490 **Sea urchin size-class and microhabitat preference**
491 Sea urchin microhabitat preference may have been associated with changes in environmental
492 conditions because the gradual decline in the occurrence of free-living *D. setosum* from autumn
493 until spring and the increase in preference for crevices during the same period (Fig. 6A, B, C)
494 closely coincides with high wave action around those months (Fig. 2A). Shelter-seeking
495 behaviors may be a response to strong hydrodynamic forces because during the calmer months in
496 summer, the occurrence of free-living sea urchins gradually increased. It is known that high
497 water motion reduces urchin movement and foraging behavior due to the threat of dislodgement
498 (*Kawamata, 1998*; *Siddon & Witman, 2003*; *Cohen-Rengifo et al., 2018*). Urchins respond to
499 increasing water motion by escaping from exposed areas and changing their outline to a more
500 streamlined shape (*Cohen-Rengifo et al., 2018*) or remain sheltered until conditions improve
501 (*Yusa & Yamamoto, 1994*; *Tamaki, Muraoka & Inoue, 2018*). In addition, *D. savignyi*, a closely
502 related Diadematid species shows a similar pattern in preferring crevices in the deep IH but only
503 few individuals were found. In the entire VH, *D. savignyi* were mostly crevice dwellers
504 throughout the study period. We speculate that although Diadematid urchins (i.e., *D. setosum* and
505 *D. savignyi*) occupy the same guild, *D. setosum* was a better competitor for resources resulting in
506 a skewed population in favor of *D. setosum*. For *H. crassispina*, this species generally prefers
507 crevices throughout both habitats except in calm conditions where they may leave their crevices
508 as in the shallow IH but also to a lesser extent in the shallow VH. Very few sea urchins of all
509 species were found in pits along the deep VH and IH (Fig. 6A, C) because pit microhabitats were
510 scarce in these areas. Overall, it was clear that the IH was mostly composed of small and
511 medium sized urchins while there was a higher chance of observing larger individuals in the VH,
512 especially for *D. savignyi* and *D. setosum*, probably due to the food availability. A study on
513 interactions between *Echinometra mathaei*, *D. savignyi* and *D. setosum* in a coral reef shows that
514 among Diadematid urchins, the body size characteristics and sedentary habits of *D. savignyi*
515 enabled it to outcompete *D. setosum* for microhabitat refuge while *E. mathaei* was the top
516 competitor for crevice microhabitats due to settlement success while benefiting greatly from
517 living in crevices because of high predation pressure compared to Diadematid urchins
518 (*McClanahan, 1988*). In our study, we suspected that the sedentary habit of *D. savignyi* was a

519   disadvantage particularly in areas where resources were scarce. In these conditions, active
520   foraging is better suited to maximize encountering food and refuge. Since our surveys were done
521   in the daytime, we were not able to observe urchin foraging at night when they are most active
522   (*Tuya, Martin & Luque, 2004*). Among the three species, *H. crassispina* was the exception,
523   because it primarily preferred crevices while rates of being free-living occurred only in the
524   shallow IH where wave action was less. A good example of this scenario is in Hong Kong where
525   *H. crassispina* form destructive feeding fronts in sheltered bays (*Urriago Suarez et al., 2021*).
526
527   According to historical records, *D. setosum* was implicated in the loss of seaweed beds in Japan
528   since the late 1800's (*Fujita, 2010*) and are regularly culled as a first step in the rehabilitation of
529   barren areas (*Nanri et al., 2011*; *Ohmura, Watanabe & Fujita, 2011*). Unlike other species,
530   Diadematid urchins have lesser commercial value in Japan due to the higher ratios of bitter
531   tasting compounds in their gonads (*Kaneko et al., 2009*) while their optimal season occurs only
532   in June (*Kaneko et al., 2012*). In our study, sea urchin densities in both habitats were low relative
533   to thresholds necessary to trigger a forward phase shift (Fig. 8), but were enough in some months
534   to maintain the barren state (Fig. 8, shallow VH, Aug. – Oct.) or even support recovery (Fig. 8,
535   deep IH) (*Ishikawa, Maegawa & Kurashima, 2016*; *Kriegisch et al., 2016*; *Ishikawa &*
536   *Kurashima, 2020*). Sea urchin barrens are known for their inherent stability since thresholds for
537   macroalgal recovery (reverse shift) is different from the one which initiated the shift (forward
538   shift) (*Filbee-Dexter & Scheibling, 2014*). The environmental conditions in the IH may be
539   contributing to unfavorable conditions for algal growth despite having lower urchin densities
540   compared to the VH.
541
542   A meta-analysis of studies on macroalgal bed-to-barren regime shifts found that sea urchin
543   biomass over 668 g m^{-2} led to overgrazing while about 34 – 71 g m^{-2} allows for macroalgal
544   recovery (*Ling et al., 2015*). Based on these estimates, the sea urchin biomass in our transects
545   were at the lower limits of those that were reported. However, the sea urchin biomass in our
546   study could be underestimating the actual values because sea urchin weights were inferred by
547   sampling a few individuals in the spring. Sea urchin reproductive cycles are marked by distinct
548   events that affect their overall biomass. For example, gonadal development and maturation and
549   the high availability of algal food lead to increasing body mass in the winter and spring, while
550   spawning and the low macroalgal diversity in the summer to autumn lead to lower body weights
551   (*Kaehler & Kennish, 1996*; *Horii, 1997*; *Bronstein, Kroh & Loya, 2016*; *Urriago et al., 2016*).
552   Hence, we suggest considering sea urchin density as an indicator for estimating the risk of phase
553   shifts as biomass is dependent on season. The Arikawa Bay Fisheries Cooperative that manages
554   the fisheries rights of the study area has indicated that sea urchin culling and harvesting has not
555   occurred at our study sites prior to or during this study.
556
557   **Sea urchin movement patterns**

558 In terms of sea urchin movement patterns, we demonstrated how sympatric sea urchin species
559 behaved differently in adjacent habitats. Generally, both taxa were more active and displaced
560 farther over a 24 h period in the IH where wave action and benthic rugosity was low, compared
561 to the VH. The displacement GLM showed a higher displacement occurring after the second
562 recapture compared to the first recapture period (Fig. 7A), indicating both species were
563 nocturnal. A study on *Diadema antillarum*, show nocturnal foraging behaviors and site fidelity
564 among the tagged urchins (*Tuya, Martin & Luque, 2004*). However, we were not able to
565 determine whether *D. setosum* displayed homing behaviors during our tagging study. We
566 interpret the sea urchin movements as a response to wave action and as foraging behavior. The
567 lower wave action and the relative food scarcity prompted urchins to forage more in the IH,
568 whereas the necessity to forage further was less at VH where waves were stronger and food was
569 relatively abundant. A number of studies document the flexibility of sea urchin diets to include
570 detritus and animal matter when algal food is low (*Freeman, 2003*; *Wangensteen et al., 2011*;
571 *Rodríguez-Barreras et al., 2015*; *Umezu et al., 2017*; *Camps-Castellà, Romero & Prado, 2020*).
572 When food was abundant, sea urchins have been known to subsist on drift algae (*Kelly,
573 Krumhansl & Scheibling, 2012*; *Kriegisch et al., 2019*; *Rennick et al., 2022*), reducing the need
574 to forage far from their refuge which indirectly reduces feeding pressure on the existing seaweed
575 beds. It is also known that the threat of predation induces alarm responses among several species
576 of sea urchins (*Snyder & Snyder, 1970*; *Campbell et al., 2001*; *Morishita & Barreto, 2011*).
577 Recent studies have found that sea urchin response to predator cues may vary depending on
578 species. For example, when a dead conspecific was present, *Strongylocentrotus intermedius*
579 formed aggregations while *Mesocentrotus nudus* responded by leaving the vicinity (*Zhadan and
580 Vaschenko, 2019*). There is also some evidence that for species like *Echinometra mathaei* (*Hart
581 and Chia, 1990*) and *H. crassispina* (*Belleza et al., 2021*), starvation weakens the anti-predator
582 response and prioritizes foraging behaviors, but not in *M. nudus* (*Chi et al., 2021*).
583
584 As for the patterns observed with the changes in urchin aggregations, the group-size GLM shows
585 that all *H. crassispina* remained solitary throughout the study. There was a net decrease in *D.
586 setosum* group-size in both habitats after the first recapture and a subsequent increase in group-
587 size after the second recapture in the IH but not in the VH (Fig. 7B). Furthermore, it is important
588 to note that *D. setosum* group sizes in the IH were similar while there were large variations in
589 group composition among experimental trials in the VH. We suspect that the high availability of
590 food and refuge in the VH supported higher recruitment survivability and safety from predation,
591 although the level of predation pressure on sea urchins in both habitats remains unclear. It is
592 known that aggregation behavior is one strategy to deter predators (*Garnick, 1978*) and are
593 maintained by close spine contact between members of the group while increased spine
594 movement indicates defensive activity against a potential predator (*Morishita & Barreto, 2011*).
595 Nevertheless, tagging activities tend to disrupt aggregations when an individual is taken from the
596 group. The tagging procedure was invasive and involved puncturing a 0.5 mm hole on the sea
597 urchin's test at the inter-ambulacral region to insert the tag. Even though the tagging injury is

598 small, urchin coelomic fluids may still leak out and evoke a flee response from the surrounding
599 urchins when the tagged urchin is returned to the group (*Campbell et al., 2001*; *Morishita &*
600 *Barreto, 2011*; *Spyksma, Shears & Taylor, 2020*). This may help explain the reduction in group
601 size in the first recapture. After the second recapture, the tagged *D. setosum* may have partially
602 healed and retained some group members or have encountered other aggregations while foraging
603 at night. This phenomenon has been observed in the Solomon Islands where *D. setosum* and *D.*
604 *savignyi* aggregations are constantly changing in size, and aggregations of both species often
605 combine (*Pearse & Arch, 1969*). In the IH, we expect sea urchin aggregations to encounter other
606 groups easily in the flat terrain but not in the VH where abundant crevices and wave action
607 results in more dynamic group interactions. Furthermore, the relative abundance of food in the
608 VH reduces the necessity to forage further.
609
610 **Past records and future implications**
611 While the importance of sea urchins as key drivers of ecosystem states is generally recognized, it
612 is equally important to note environmental changes that occurred in recent years. A fisheries
613 survey in 1991 shows that VH was once a vibrant algal bed that included 5 species of
614 *Sargassum*, 3 subtropical kelp species and about 4 species of abalone and several commercially
615 important fish species (*Nagasaki Prefecture Fisheries Development Association, 1991*). There
616 were no official records of surveys done at IH but remote sensing maps available through the
617 Geospatial Information Authority of Japan
618 (https://www.gsi.go.jp/johofukyu/johofukyu210322.html), shows that IH was once possibly
619 vegetated in the late 1960's prior to coastal armoring and the construction of the concrete jetty in
620 the early 1970's (Fig. 9), given its proximity to areas previously surveyed (*Nagasaki Prefecture*
621 *Fisheries Development Association, 1991*). Urbanization and coastal development are known
622 anthropogenic stressors that affect shallow subtidal ecosystems (*Kevekordes, 2001*; *Coleman et*
623 *al., 2008*; *Coleman & Wernberg, 2017*). In particular, coastal armoring in Japan has been used
624 extensively as a response to coastal erosion, sea level rise, and storm surge (*Koike, 1996*).
625 Ironically, a trade-off occurs as natural habitats are lost for coastal protection. In this case, we
626 speculate that coastal development has contributed to the loss of a seaweed habitat by altering
627 the area's hydrodynamic conditions leading to increased sedimentation (*Airoldi, 1998, 2003*).
628 Furthermore, the average winter temperature in Arikawa Bay appear to have increased and
629 remained elevated since 2018 (Fig. 10, *GN Nishihara, 2021, unpublished data*). Higher winter
630 temperatures mean sea urchins (*Ishikawa and Kurashima, 2020*) and herbivorous fish
631 (*Yamaguchi et al., 2006*; *Noda et al., 2016*) are able to remain active and grazing pressure may
632 persist throughout the year.
633
634 **Conclusions**
635 Our study highlights the similarities and differences in the behavior and distribution of sympatric
636 sea urchins, *Diadema savignyi*, *D. setosum* and *Heliocidaris crassispina* in adjacent habitats
637 under natural conditions. We found that, (1) sea urchins show an increased preference for

638   sheltered habitats such as crevices and burrows during the months with high wave action while
639   the incidence of free-living sea urchins increased during the calmer months. (2) In areas where
640   benthic rugosity and wave action are low, sea urchins tend to displace further.
641

642   Acknowledgements

643   We thank the Arikawa Bay Fisheries Cooperative for providing resources and cooperation which
644   allowed us to conduct the study.

645

646   References

Agnetta D, Bonaviri C, Badalamenti F, Scianna C, Vizzini S, Gianguzza P. 2013. Functional traits of two co-occurring sea urchins across a barren/forest patch system. *Journal of Sea Research*, 76, pp. 170–177. Available at: https://doi.org/10.1016/j.seares.2012.08.009.

Airoldi L. 1998. Roles of disturbance, sediment stress, and substratum retention on spatial dominance in algal turf. *Ecology*, 79(8), pp. 2759–2770. Available at: https://doi.org/10.1890/0012-9658(1998)079[2759:RODSSA]2.0.CO;2.

Airoldi L. 2003. The effects of sedimentation on rocky coastal assemblages. *Oceanography and Marine Biology: an Annual Review*, 41, pp. 161–236.

Barthelme S, Tschumperle D, Wijffels J, Edine J, Ochi S. 2021. imager: Image processing library based on "CImg" (0.42.11). Available at: https://github.com/dahtah/imager/.

Belleza D, Kawabata Y, Toda T, Nishihara GN. 2021. Effects of dead conspecifics, hunger states, and seasons on the foraging behavior of the purple urchin *Heliocidaris crassispina*. *Marine Ecology Progress Series*, 664, pp. 133–148. Available at: https://doi.org/10.3354/meps13653.

Benedetti-Cecchi L, Pannacciulli F, Bulleri F, Moschella PS, Airoldi L, Relini G, Cinelli F. 2001. Predicting the consequences of anthropogenic disturbance: large-scale effects of loss of canopy algae on rocky shores. *Marine Ecology Progress Series*, 214, pp. 137–150. Available at: https://doi.org/10.3354/meps214137.

Bonaviri C, Vega Fernandez T, Fanelli G, Badalamenti F, Gianguzza P. 2011. Leading role of the sea urchin *Arbacia lixula* in maintaining the barren state in southwestern Mediterranean. *Marine Biology*, 158(11), pp. 2505–2513. Available at: https://doi.org/10.1007/s00227-011-1751-2.

Bronstein O, Kroh A, Loya Y. 2016. Reproduction of the long-spined sea urchin *Diadema setosum* in the Gulf of Aqaba - implications for the use of gonad-indexes. *Scientific Reports*, 6(1), p. 29569. Available at: https://doi.org/10.1038/srep29569.

Bürkner PC. 2017. brms : An *R* package for Bayesian multilevel models using *Stan*. *Journal of Statistical Software*, 80(1). Available at: https://doi.org/10.18637/jss.v080.i01.

Bürkner PC. 2018. Advanced Bayesian multilevel modeling with the *R* package brms. *The R Journal*, 10(1), p. 395. Available at: https://doi.org/10.32614/RJ-2018-017.

Campbell AC, Coppard S, D'Abreo C, Tudor-Thomas R. 2001. Escape and aggregation responses of three echinoderms to conspecific stimuli. *The Biological Bulletin*, 201(2), pp. 175–185. Available at: https://doi.org/10.2307/1543332.

Camps-Castellà J, Romero J, Prado P. (2020) 'Trophic plasticity in the sea urchin *Paracentrotus lividus*, as a function of resource availability and habitat features', *Marine Ecology Progress Series*, 637, pp. 71–85. Available at: https://doi.org/10.3354/meps13235.

Carpenter SR, Ludwig D, Brock WA. 1999. Management of eutrophication for lakes subject to potentially irreversible change. *Ecological Applications*, 9(3), pp. 751–771. Available at: https://doi.org/10.1890/1051-0761(1999)009[0751:MOEFLS]2.0.CO;2.

Chen H. 2019. Bayesian inference of environmental effects on seaweed production in Japan via a production-environmental suitability model. *Botanical Studies*, 60(1), pp. 1–10. Available at: https://doi.org/10.1186/s40529-018-0250-x.

Chenelot H, Jewett SC, Hoberg MK. 2011. Macrobenthos of the nearshore Aleutian Archipelago, with emphasis on invertebrates associated with *Clathromorphum nereostratum* (Rhodophyta, Corallinaceae). *Marine Biodiversity*, 41(3), pp. 413–424. Available at: https://doi.org/10.1007/s12526-010-0071-y.

Chi X, Yang M, Hu F, Huang X, Yu Y, Chang Y, Wang Q, Zhao C. 2021. Foraging behavior of the sea urchin *Mesocentrotus nudus* exposed to conspecific alarm cues in various conditions. *Scientific Reports*, 11:15654. Available at: https://doi.org/10.1038/s41598-021-94969-w.

Clements JC, Dupont S, Jutfelt F. 2021. "Urchin pinning": Behavioural observations reveal how hungry urchins actively prey upon their sea star predators. *Ethology*, 127(6), pp. 484–489. Available at: https://doi.org/10.1111/eth.13147.

Cohen-Rengifo M, Agüera A, Detrain C, Bouma TJ, Dubois P, Flammang P. 2018. Biomechanics and behaviour in the sea urchin *Paracentrotus lividus* (Lamarck, 1816) when facing gradually increasing water flows. *Journal of Experimental Marine Biology and Ecology*, 506, pp. 61–71. Available at: https://doi.org/10.1016/j.jembe.2018.05.010.

Coleman MA, Kelaher BP, Steinberg PD, Millar AJK. 2008. Absence of large brown macroalga on urbanized rocky reefs around Sydney, Australia, and evidence for historical decline. *Journal of Phycology*, 44(4), pp. 897–901. Available at: https://doi.org/10.1111/j.1529-8817.2008.00541.x.

Coleman MA, Wernberg T. 2017. Forgotten underwater forests: The key role of fucoids on Australian temperate reefs. *Ecology and Evolution*, 7(20), pp. 8406–8418. Available at: https://doi.org/10.1002/ece3.3279.

Contreras S, Castilla J. 1987. Feeding behavior and morphological adaptations in two sympatric sea urchin species in central Chile. *Marine Ecology Progress Series*, 38, pp. 217–224. Available at: https://doi.org/10.3354/meps038217.

Eger AM, Marzinelli EM, Christie H, Fagerli CW, Fujita D, Gonzalez AP, Hong SW, Kim, JH, Lee LC, McHugh TA, Nishihara GN, Tatsumi M, Steinberg PD, Verges A. 2022. Global kelp forest restoration: past lessons, present status, and future directions. *Biological Reviews*, 97(4), pp. 1449–1475. Available at: https://doi.org/10.1111/brv.12850.

Estes JA, Palmisano JF. 1974. Sea otters: Their role in structuring nearshore communities. *Science*, 185(4156), pp. 1058–1060. Available at: https://doi.org/10.1126/science.185.4156.1058.

Filbee-Dexter K, Scheibling R. 2014. Sea urchin barrens as alternative stable states of collapsed kelp ecosystems. *Marine Ecology Progress Series*, 495, pp. 1–25. Available at: https://doi.org/10.3354/meps10573.

Flukes E, Johnson C, Ling S. 2012. Forming sea urchin barrens from the inside out: an alternative pattern of overgrazing. *Marine Ecology Progress Series*, 464, pp. 179–194. Available at: https://doi.org/10.3354/meps09881.

Freeman SM. 2003. Size-dependent distribution, abundance and diurnal rhythmicity patterns in the short-spined sea urchin *Anthocidaris crassispina*. *Estuarine, Coastal and Shelf Science*, 58(4), pp. 703–713. Available at: https://doi.org/10.1016/S0272-7714(03)00134-3.

Frey D, Gagnon P. 2016. Spatial dynamics of the green sea urchin *Strongylocentrotus droebachiensis* in food-depleted habitats. *Marine Ecology Progress Series*, 552, pp. 223–240. Available at: https://doi.org/10.3354/meps11787.

Fujita D. 2010. Current status and problems of isoyake in Japan. *Bulletin of the Fisheries Research Agency*, 32, pp. 33–42.

Fujita D, Ogata R, Akita S, Takagi K, Yamada H. 2013. Are there any top-down controls in *Diadema* barrens in the warm temperate Pacific coasts of Japan? *Cahiers de Biologie Marine*, pp. 615–624.

Garnick E. 1978. Behavioral ecology of *Strongylocentrotus droebachiensis* (Muller) (Echinodermata: Echinoidea): Aggregating behavior and chemotaxis. *Oecologia*, 37(1), pp. 77–84. Available at: https://doi.org/10.1007/BF00349993.

Gauna MC, Cáceres EJ, Parodi ER. 2013. Temporal variations of vegetative features, sex ratios and reproductive phenology in a *Dictyota dichotoma* (Dictyotales, Phaeophyceae) population of Argentina. *Helgoland Marine Research*, 67(4), pp. 721–732. Available at: https://doi.org/10.1007/s10152-013-0357-0.

Gelman A, Simpson D, Betancourt M. 2017. The prior can often only be understood in the context of the likelihood. *Entropy*, 19(10), pp. 1–13. Available at: https://doi.org/10.3390/e19100555.

Graham MH. 2010. Comparisons between East-Asian isoyake and deforestation in global kelp systems. *Bulletin of the Fisheries Research Agency*, 32, pp. 47–50.

Gravem SA, Adams NL. 2012. Sex and microhabitat influence the uptake and allocation of mycosporine-like amino acids to tissues in the purple sea urchin, *Strongylocentrotus purpuratus*. *Marine Biology*, 159(12), pp. 2839–2852. Available at: https://doi.org/10.1007/s00227-012-2045-z.

Gregr EJ, Christensen V, Nichol L, Martone RG, Markel RW, Watson JC, Harley CDG, Pakhomov EA, Shurin JB, Chan KMA. 2020. Cascading social-ecological costs and benefits triggered by a recovering keystone predator. *Science*, 368(6496), pp. 1243–1247. Available at: https://doi.org/10.1126/science.aay5342.

Guidetti P, Dulčić J. 2007. Relationships among predatory fish, sea urchins and barrens in Mediterranean rocky reefs across a latitudinal gradient. *Marine Environmental Research*, 63(2), pp. 168–184. Available at: https://doi.org/10.1016/j.marenvres.2006.08.002.

Haroun RJ, Yokohama Y, Aruga, Y. 1989. Annual growth cycle of the brown alga *Ecklonia cava* in central Japan. *Scientia Marina*, 53(2), pp. 349–356.

Hart, LJ, Chia F-S. 1990. Effect of food supply and body size on the foraging behavior of the burrowing sea urchin *Echinometra mathaei* (de Blainville). *Journal of Experimental Marine Biology and Ecology*, 135, pp. 99-108.

Horii T. 1997. The annual reproductive cycle and lunar spawning rhythms of the purple sea urchin *Anthocidaris crassispina*. *Nippon Suisan Gakkaishi*, 63(1), pp. 17–22. Available at: https://doi.org/10.2331/suisan.63.17. [in Japanese with English abstract].

Ishikawa T, Kurashima A. 2020. Estimation of the feeding pressure of a sea urchin (*Diadema setosum*) population on a barren ground in a temperate region of Japan. *Plankton and Benthos Research*, 15(2), pp. 112–120. Available at: https://doi.org/10.3800/pbr.15.112.

Ishikawa T, Maegawa M, Kurashima, A. 2016. Effect of sea urchin (*Diadema setosum*) density on algal composition and biomass in cage experiments. *Plankton and Benthos Research*, 11(4), pp. 112–119. Available at: https://doi.org/10.3800/pbr.11.112.

Kaehler S, Kennish R. 1996. Summer and winter comparisons in the nutritional value of marine macroalgae from Hong Kong. *Botanica Marina*, 39(1–6). Available at: https://doi.org/10.1515/botm.1996.39.1-6.11.

Kaneko K, Shirai T, Tanaka M, Kamei M, Matsumoto H, Osako K. 2009. Taste characteristics of the gonad of longspine black urchin *Diadema setosum*. *Nippon Suisan Gakkaishi*, 75(4), pp. 689–694. Available at: https://doi.org/10.2331/suisan.75.689. [in Japanese with English abstract].

Kaneko K, Matsumoto H, Shirai T, Kamei M, Okazaki E, Osako K. 2012. Seasonal variations in free amino acid composition and taste aspects of black sea urchin, *Diadema setosum*, gonad.

Food Science and Technology Research, 18(6), pp. 835–842. Available at:
https://doi.org/10.3136/fstr.18.835.

Kawamata S. 1998. Effect of wave-induced oscillatory flow on grazing by a subtidal sea urchin *Strongylocentrotus nudus* (A. Agassiz). *Journal of Experimental Marine Biology and Ecology*, 224(1), pp. 31–48. Available at: https://doi.org/10.1016/S0022-0981(97)00165-2.

Kawamata S, Taino S, Miyaji M, Nakamura Y. 2016. Size-selective predation on the sea urchin *Echinometra* sp. A by Japanese spiny lobster *Panulirus japonicus*. *Nippon Suisan Gakkaishi*, 82(3), pp. 306–314. Available at: https://doi.org/10.2331/suisan.15-00057. [in Japanese with English abstract].

Kelly J, Krumhansl K, Scheibling R. 2012. Drift algal subsidies to sea urchins in low-productivity habitats. *Marine Ecology Progress Series*, 452, pp. 145–157. Available at: https://doi.org/10.3354/meps09628.

Kevekordes K. 2001. Toxicity tests using developmental stages of *Hormosira banksii* (Phaeophyta) identify ammonium as a damaging component of secondary treated sewage effluent discharged into Bass Strait, Victoria, Australia. *Marine Ecology Progress Series*, 219, pp. 139–148. Available at: https://doi.org/10.3354/meps219139.

Koike K. 1996. The countermeasures against coastal hazards in Japan. *GeoJournal*, 38(3). Available at: https://doi.org/10.1007/BF00204722.

Kriegisch N, Reeves S, Johnson CR, Ling SD, Russell BD. 2016. Phase-shift dynamics of sea urchin overgrazing on nutrified reefs. *PLoS ONE*, 11(12), p. e0168333. Available at: https://doi.org/10.1371/journal.pone.0168333.

Kriegisch N, Reeves SE, Flukes EB, Johnson CR, Ling SD. 2019. Drift-kelp suppresses foraging movement of overgrazing sea urchins. *Oecologia*, 190(3), pp. 665–677. Available at: https://doi.org/10.1007/s00442-019-04445-6.

Krumhansl KA, Okamoto DK, Rassweiler A, Novak M, Bolton JJ, Cavanaugh KC, Connell SD, Johnson CR, Konar B, Ling SD, Micheli F, Norderhaug KM, Pérez-Matus A, Sousa-Pinto I, Reed DC, Salomon AK, Shears NT, Wernberg T, Anderson RJ, Barrett NS, Buschmann AH, Carr MH, Caselle JE, Derrien-Courtel S, Edgar GJ, Edwards M, Estes JA, Goodwin C, Kenner MC, Kushner DJ, Moy FE, Nunn J, Steneck RS, Vásquez J, Watson J, Witman JD, Byrnes JEK. 2016. Global patterns of kelp forest change over the past half-century. *Proceedings of the National Academy of Sciences*, 113(48), pp. 13785–13790. Available at: https://doi.org/10.1073/pnas.1606102113.

Lauzon-Guay J, Scheibling R, Barbeau M. 2009. Modelling phase shifts in a rocky subtidal ecosystem. *Marine Ecology Progress Series*, 375, pp. 25–39. Available at: https://doi.org/10.3354/meps07758.

Leclerc J-C, de Bettignies T, de Bettignies F, Christie H, Franco JN, Leroux C, Davoult D, Pedersen MF, Filbee-Dexter K, Wernberg T. 2021. Local flexibility in feeding behaviour and

contrasting microhabitat use of an omnivore across latitudes. *Oecologia*, 196(2), pp. 441–453. Available at: https://doi.org/10.1007/s00442-021-04936-5.

Lee HH, Kim C-H. 2013. Long-term variability of sea surface temperature in the East China Sea: A review. *Ocean and Polar Research*, 35(2), pp. 171–179. Available at: https://doi.org/10.4217/OPR.2013.35.2.171. [in Korean with English abstract].

LeGault K, Hunt H. 2016. Cannibalism among green sea urchins *Strongylocentrotus droebachiensis* in the laboratory and field. *Marine Ecology Progress Series*, 542, pp. 1–12. Available at: https://doi.org/10.3354/meps11564.

Lewin W-C, Freyhof J, Huckstorf V, Mehner T, Wolter C. 2010. When no catches matter: Coping with zeros in environmental assessments. *Ecological Indicators*, 10, pp. 572-583.

Ling SD, Scheibling RE, Rassweiler A, Johnson CR, Shears N, Connell SD, Salomon AK, Norderhaug KM, Pérez-Matus A, Hernández JC, Clemente S, Blamey LK, Hereu B, Ballesteros E, Sala E, Garrabou J, Cebrian E, Zabala M, Fujita D, Johnson LE. 2015. Global regime shift dynamics of catastrophic sea urchin overgrazing. *Philosophical Transactions of the Royal Society B: Biological Sciences*, 370(1659), p. 20130269. Available at: https://doi.org/10.1098/rstb.2013.0269.

Littler MM, Murray SN. 1975. Impact of sewage on the distribution, abundance and community structure of rocky intertidal macro-organisms. *Marine Biology*, 30(4), pp. 277–291. Available at: https://doi.org/10.1007/BF00390633.

Matsumoto K, Sasai Y, Sasaoka K, Siswanto E, Honda MC. 2021. The formation of subtropical phytoplankton bloom is dictated by water column stability during winter and spring in the oligotrophic northwestern North Pacific. *Journal of Geophysical Research: Oceans*, 126, e2020JC016864, pp. 1-18. Available at: https://doi.org/10.1029/2020JC016864.

Martínez B, Pato LS, Rico JM. 2012. Nutrient uptake and growth responses of three intertidal macroalgae with perennial, opportunistic and summer-annual strategies. *Aquatic Botany*, 96(1), pp. 14–22. Available at: https://doi.org/10.1016/j.aquabot.2011.09.004.

McClanahan TR. 1988. Coexistence in a sea urchin guild and its implications to coral reef diversity and degradation. *Oecologia*, 77(2), pp. 210–218. Available at: https://doi.org/10.1007/BF00379188.

McKay K, Heck, K. 2008. Presence of the Jonah crab *Cancer borealis* significantly reduces kelp consumption by the green sea urchin *Strongylocentrotus droebachiensis*. *Marine Ecology Progress Series*, 356, pp. 295–298. Available at: https://doi.org/10.3354/meps07238.

McManus JW, Polsenberg JF. 2004. Coral–algal phase shifts on coral reefs: Ecological and environmental aspects. *Progress in Oceanography*, 60(2–4), pp. 263–279. Available at: https://doi.org/10.1016/j.pocean.2004.02.014.

Morishita V, Barreto R. 2011. Black sea urchins evaluate predation risk using chemical signals from a predator and injured con- and heterospecific prey. *Marine Ecology Progress Series*, 435, pp. 173–181. Available at: https://doi.org/10.3354/meps09253.

Nagasaki Prefecture Fisheries Development Association. 1991. A survey report on fisheries resources and fishing grounds at Arikawa Town. Nagasaki Prefecture, pp. 70. [in Japanese].

Nanri K, Nakajima Y, Yatsuya K, Kiyomoto S, Andou W, Yoshimura T. 2011. Some approaches for the recovery from barren grounds in Shin-Mie, Nagasaki Prefecture. *Fisheries Engineering*, 48(1), pp. 59–64. [in Japanese with English abstract].

Noda M, Kawano M, Okamoto K, Murase N. 2016. Estimation of daily feeding rate and diel feeding rhythm of herbivorous fish *Kyphosus bigibbus* in captivity. *Journal of National Fisheries University*, 64(4), pp. 219–225. [in Japanese with English abstract].

Nyström M, Folke C, Moberg F. 2000. Coral reef disturbance and resilience in a human-dominated environment. *Trends in Ecology & Evolution*, 15(10), pp. 413–417. Available at: https://doi.org/10.1016/S0169-5347(00)01948-0.

Ohmura H, Watanabe S, Fujita D. 2011. The reforestation on urchin barrens in Onagawa Bay, Miyagi Prefecture. *Fisheries Engineering*, 48(1), pp. 35–39. [in Japanese with English abstract].

Ooms J. 2021. magick: Advanced graphics and image-processing in *R*. R package version 2.7.3. Available at: https://CRAN.R-project.org/package=magick (R package version 2.7.3).

Pearse JS, Arch SW. 1969. The aggregation behavior of *Diadema* (Echinodermata, Echinoidea). *Micronesica*, 5, pp. 165–171.

Pessarrodona A, Filbee-Dexter K, Alcoverro T, Boada J, Feehan CJ, Fredriksen S, Grace SP, Nakamura Y, Narvaez CA, Norderhaug KM, Wernberg T. 2021. Homogenization and miniaturization of habitat structure in temperate marine forests. *Global Change Biology*, 27(20), pp. 5262–5275. Available at: https://doi.org/10.1111/gcb.15759.

Poore AGB, Campbell AH, Coleman RA, Edgar GJ, Jormalainen V, Reynolds PL, Sotka EE, Stachowicz JJ, Taylor RB, Vanderklift MA, Duffy JE. 2012. Global patterns in the impact of marine herbivores on benthic primary producers. *Ecology Letters*, 15(8), pp. 912–922. Available at: https://doi.org/10.1111/j.1461-0248.2012.01804.x.

Preskitt LB, Vroom PS, Smith CM. 2004. A rapid ecological assessment (REA) quantitative survey method for benthic algae using photoquadrats with SCUBA. *Pacific Science*, 58(2), pp. 201–209. Available at: https://doi.org/10.1353/psc.2004.0021.

Provost EJ, Kelaher BP, Dworjanyn SA, Russell BD, Connell SD, Ghedini G, Gillanders BM, Figueira W, Coleman MA. 2017. Climate-driven disparities among ecological interactions threaten kelp forest persistence. *Global Change Biology*, 23(1), pp. 353–361. Available at: https://doi.org/10.1111/gcb.13414.

R Core Team. 2022. *R*: A language and environment for statistical computing. R Foundation for Statistical Computing. Available at: https://www.R-project.org/.

Rennick M, DiFiore BP, Curtis J, Reed DC, Stier AC. 2022. Detrital supply suppresses deforestation to maintain healthy kelp forest ecosystems. *Ecology*, 103(5). Available at: https://doi.org/10.1002/ecy.3673.

Risk MJ. 1972. Fish diversity on a coral reef in the Virgin Islands. *Atoll Research Bulletin*, (153), pp. 1–7.

Rodríguez-Barreras R, Cuevas E, Cabanillas-Terán N, Sabat AM. 2015. Potential omnivory in the sea urchin *Diadema antillarum*?. *Regional Studies in Marine Science*, 2, pp. 11–18. Available at: https://doi.org/10.1016/j.rsma.2015.08.005.

Rodríguez-Barreras R, Sabat AM. 2015. Evaluation of three tagging methods in the sea urchin *Diadema antillarum*. *Journal of the Marine Biological Association of the United Kingdom*, 95(6), pp. 1255–1260. Available at: https://doi.org/10.1017/S0025315415000302.

Sato Y, Nishihara GN, Tanaka A, Belleza DFC, Kawate A, Inoue Y, Hinode K, Matsuda Y, Tanimae S, Tozaki K, Terada R, Endo H. 2022. Variability in the net ecosystem productivity (NEP) of seaweed farms. *Frontiers in Marine Science*, 9, p. 861932. Available at: https://doi.org/10.3389/fmars.2022.861932.

Scheffer M, Hosper SH, Meijer M-L, Moss B, Jeppesen E. 1993. Alternative equilibria in shallow lakes. *Trends in Ecology & Evolution*, 8(8), pp. 275–279. Available at: https://doi.org/10.1016/0169-5347(93)90254-M.

Scheffer M, Carpenter S, Foley JA, Folke C, Walker B. 2001. Catastrophic shifts in ecosystems. *Nature*, 413(6856), pp. 591–596. Available at: https://doi.org/10.1038/35098000.

Serisawa Y, Imoto Z, Ishikawa T, Ohno M. 2004. Decline of the *Ecklonia cava* population associated with increased seawater temperatures in Tosa Bay, southern Japan. *Fisheries Science*, 70(1), pp. 189–191. Available at: https://doi.org/10.1111/j.0919-9268.2004.00788.x.

Seymour RJ, Tegner MJ, Dayton PK, Parnell PE. 1989. Storm wave induced mortality of giant kelp, *Macrocystis pyrifera*, in Southern California. *Estuarine, Coastal and Shelf Science*, 28(3), pp. 277–292. Available at: https://doi.org/10.1016/0272-7714(89)90018-8.

Siddon C, Witman J. 2003. Influence of chronic, low-level hydrodynamic forces on subtidal community structure. *Marine Ecology Progress Series*, 261, pp. 99–110. Available at: https://doi.org/10.3354/meps261099.

Son YB, Ryu JH, Noh JH, Ju SJ, Kim S-H. 2012. Climatological variability of satellite-derived sea surface temperature and chlorophyll in the south sea of Korea and East China Sea. *Ocean and Polar Research*, 34(2), pp. 201–218. Available at: https://doi.org/10.4217/OPR.2012.34.2.201. [in Korean with English abstract].

Snyder N, Snyder H. 1970. Alarm responses of *Diadema antillarum*. *Science*, 168, pp. 276-278.

Spyksma A, Shears N, Taylor R. 2020. Injured conspecifics as an alarm cue for the sea urchin *Evechinus chloroticus*. *Marine Ecology Progress Series*, 641, pp. 135–144. Available at: https://doi.org/10.3354/meps13301.

Strain EMA, Thomson RJ, Micheli F, Mancuso FP, Airoldi L. 2014. Identifying the interacting roles of stressors in driving the global loss of canopy-forming to mat-forming algae in marine ecosystems. *Global Change Biology*, 20(11), pp. 3300–3312. Available at: https://doi.org/10.1111/gcb.12619.

Tamaki H, Muraoka D, Inoue T. 2018. Effect of water flow on grazing by the sea urchin (*Strongylocentrotus Nudus*) in the presence of refuge habitat. *Journal of Water and Environment Technology*, 16(1), pp. 30–39. Available at: https://doi.org/10.2965/jwet.17-010.

Tegner MJ, Levin LA. 1983. Spiny lobsters and sea urchins: Analysis of a predator-prey interaction. *Journal of Experimental Marine Biology and Ecology*, 73(2), pp. 125–150. Available at: https://doi.org/10.1016/0022-0981(83)90079-5.

Toste MF, Parente MA, Neto AI, Fletcher RL. 2003. Life history of *Hydroclathrus clathratus* (Scytosiphonaceae, Phaeophyta) in the Azores. *Cryptogamie Algologie*, 24(3), pp. 209–218.

Trebilco R, Dulvy NK, Stewart H, Salomon AK. 2015. The role of habitat complexity in shaping the size structure of a temperate reef fish community. *Marine Ecology Progress Series*, 532, pp. 197–211. Available at: https://doi.org/10.3354/meps11330.

Tuya F, Martin JA, Luque A. 2004. Patterns of nocturnal movement of the long-spined sea urchin *Diadema antillarum* (Philippi) in Gran Canaria (the Canary Islands, central East Atlantic Ocean). *Helgoland Marine Research*, 58(1), pp. 26–31. Available at: https://doi.org/10.1007/s10152-003-0164-0.

Umezu Y, Onitsuka T, Kawamura T, Watanabe Y. 2017. Feeding of the short-spined sea urchin *Strongylocentrotus intermedius* on macroalgae and benthic animals. *Fisheries Science*, 83(2), pp. 221–233. Available at: https://doi.org/10.1007/s12562-016-1056-y.

Urriago JD, Wong JCY, Dumont CP, Qiu J-W. 2016. Reproduction of the short-spined sea urchin *Heliocidaris crassispina* (Echinodermata: Echinoidea) in Hong Kong with a subtropical climate. *Regional Studies in Marine Science*, 8, pp. 445–453. Available at: https://doi.org/10.1016/j.rsma.2016.03.005.

Urriago Suarez JD, Wong JCY, Dumont CP, Qiu J-W. 2021. High density and secondary production but variable recruitment of a sea urchin in subtidal barren areas of Hong Kong. *Regional Studies in Marine Science*, 48, p. 102027. Available at: https://doi.org/10.1016/j.rsma.2021.102027.

Vanderklift MA, Kendrick GA, Smit AJ. 2006. Differences in trophic position among sympatric sea urchin species. *Estuarine, Coastal and Shelf Science*, 66(1–2), pp. 291–297. Available at: https://doi.org/10.1016/j.ecss.2005.09.004.

Vanderklift M, Wernberg T. 2010. Stable isotopes reveal a consistent consumer–diet relationship across hundreds of kilometres. *Marine Ecology Progress Series*, 403, pp. 53–61. Available at: https://doi.org/10.3354/meps08484.

Vehtari A, Gelman A, Gabry J. 2017. Practical Bayesian model evaluation using leave-one-out cross-validation and WAIC. *Statistics and Computing*, 27(5), pp. 1413–1432. Available at: https://doi.org/10.1007/s11222-016-9696-4.

Vergés A, Doropolous C, Malcolm HA, Skye M, Garcia-Pizá M, Marzinelli EM, Campbell AH, Ballesteros E, Hoey AS, Vila-Concejo A, Bozec Y-M, Steinberg PD. 2016. Long-term empirical evidence of ocean warming leading to tropicalization of fish communities, increased herbivory, and loss of kelp. *Proceedings of the National Academy of Sciences*, 113(48), pp. 13791–13796. Available at: https://doi.org/10.1073/pnas.1610725113.

Wang XH. 2002. Tide-induced sediment resuspension and the bottom boundary layer in an idealized estuary with a muddy bed. *Journal of Physical Oceanography*, 32(11), pp. 3113-3131. Available at: https://doi.org/10.1175/1520-0485(2002)032<3113:TISRAT>2.02.CO;2.

Wangensteen O, Turon X, García-Cisneros A, Recasens M, Romero J, Palacín C. 2011. A wolf in sheep's clothing: carnivory in dominant sea urchins in the Mediterranean. *Marine Ecology Progress Series*, 441, pp. 117–128. Available at: https://doi.org/10.3354/meps09359.

Wernberg T, Filbee-Dexter K. 2018. Grazers extend blue carbon transfer by slowing sinking speeds of kelp detritus. *Scientific Reports*, 8(1), p. 17180. Available at: https://doi.org/10.1038/s41598-018-34721-z.

Williams J, Coleman MA, Jordan A. 2020. Depth, nutrients and urchins explain variability in *Ecklonia radiata* (Laminariales) distribution and cover across ten degrees of latitude. *Aquatic Botany*, 166, p. 103274. Available at: https://doi.org/10.1016/j.aquabot.2020.103274.

Xu C, Vergnon R, Cornelissen JHC, Hantson S, Holmgren M, van Nes EH, Scheffer M. 2015. Temperate forest and open landscapes are distinct alternative states as reflected in canopy height and tree cover. *Trends in Ecology & Evolution*, 30(9), pp. 501–502. Available at: https://doi.org/10.1016/j.tree.2015.07.002.

Yamaguchi A, Inoue K, Furumitsu K, Kiriyama T, Yoshimura T, Koido T, Nakata H. 2006. Behavior and migration of rabbitfish *Siganus fuscescens* and grey seachub *Kyphosus bigibbus* off Nomozaki, Kyushu, tracked by biotelemetry method. *Nippon Suisan Gakkaishi*, 72(6), pp. 1046–1056. [in Japanese with English abstract].

Yamaguchi A, Furumitsu K, Yagishita N, Kume G. 2010. Biology of herbivorous fish in the coastal areas of western Japan. in *Coastal Environmental and Ecosystem Issues of the East China Sea*. Terrapub & Nagasaki University, pp. 181–190.

Yoshida G, Yoshikawa K, Terawaki T. 2001. Growth and maturation of two populations of *Sargassum horneri* (Fucales, Phaeophyta) in Hiroshima Bay, the Seto Inland Sea. *Fisheries Science*, 67(6), pp. 1023–1029. Available at: https://doi.org/10.1046/j.1444-2906.2001.00357.x.

Yusa Y, Yamamoto T. 1994. Inside or outside the pits : Variable mobility in conspecific sea urchin, *Anthocidaris crassispina* (A. Agassiz). *Publications of the Seto Marine Biological Laboratory*, 36(4), pp. 255–266. Available at: https://doi.org/10.5134/176235.

Zhadan PM, Vaschenko MA. 2019. Long-term study of behaviors of two cohabiting sea urchin species, *Mesocentrotus nudus* and *Strongylocentrotus intermedius*, under conditions of high food quantity and predation risk in situ. *PeerJ*, 7. DOI 10.7717/peerj.8087.

Figure 1

Study site map.

Map of the Goto Islands showing the location of Arikawa Bay and the study sites (inset) monitored in the study.
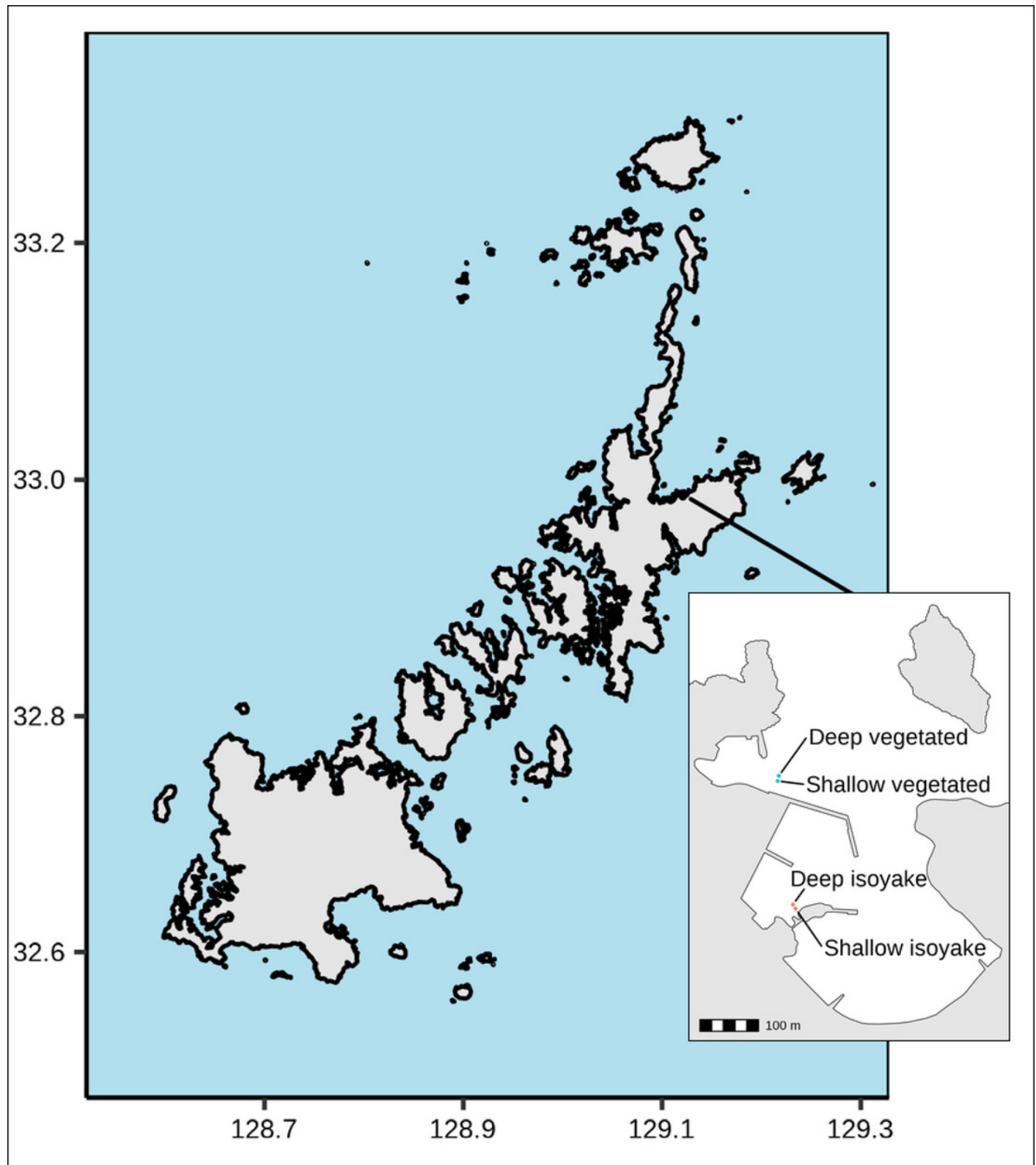
Figure 2

The environmental data recorded by instruments during the study.

The monthly daily average (A) wave heights, (B) light levels (PPFD), and (C) temperature from the isoyake habitat and vegetated habitat. The points are the observations, the solid and dashed lines are the expectations of the generalized additive models and the shaded regions indicate the 95% highest density credible interval.
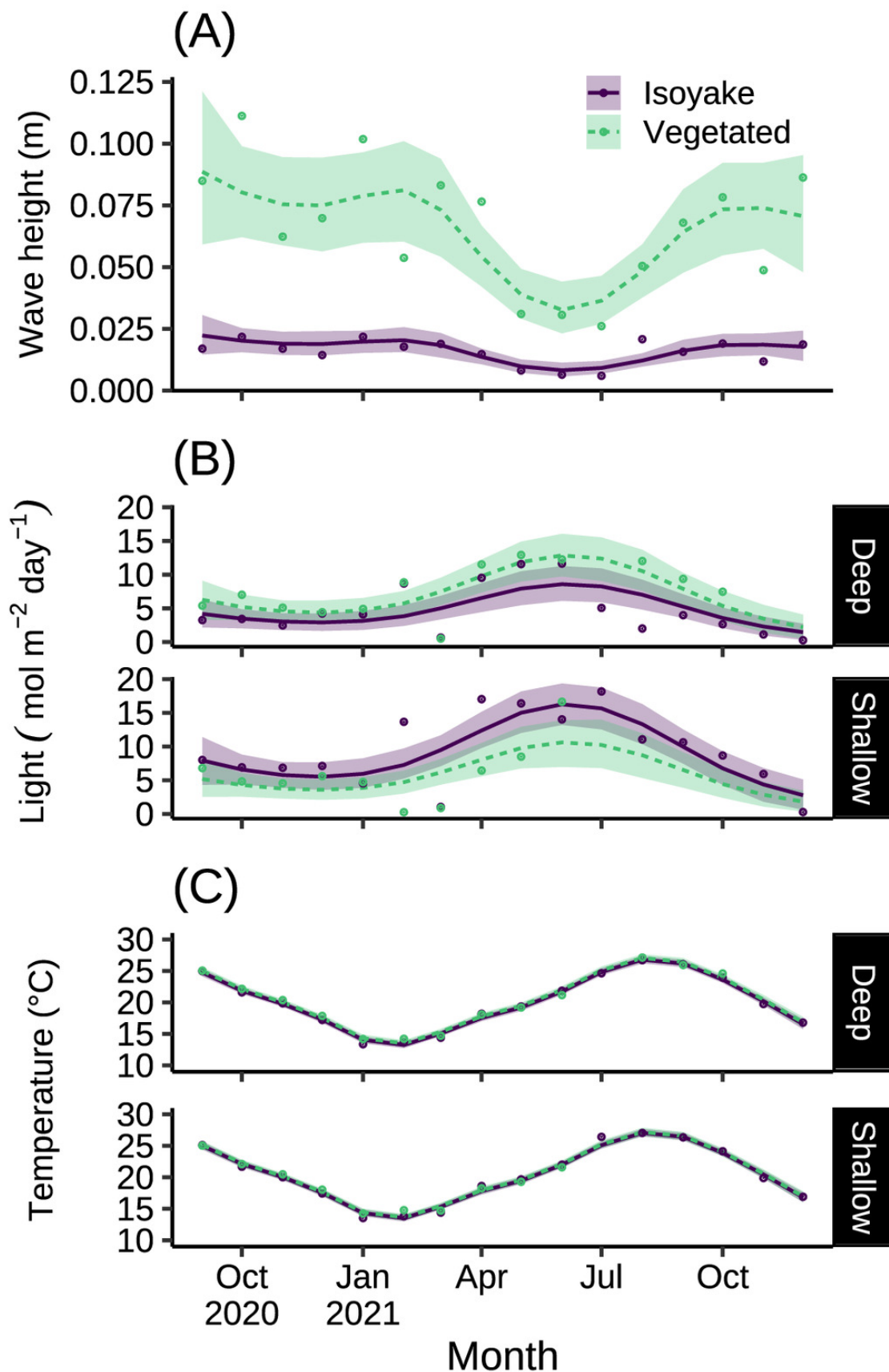
Figure 3

The benthic rugosity at the isoyake habitat and vegetated habitat.

The pale-colored points indicate the observations while the solid points are the mean expected rugosity of the generalized linear model and the vertical lines are the 95% highest density credible interval.
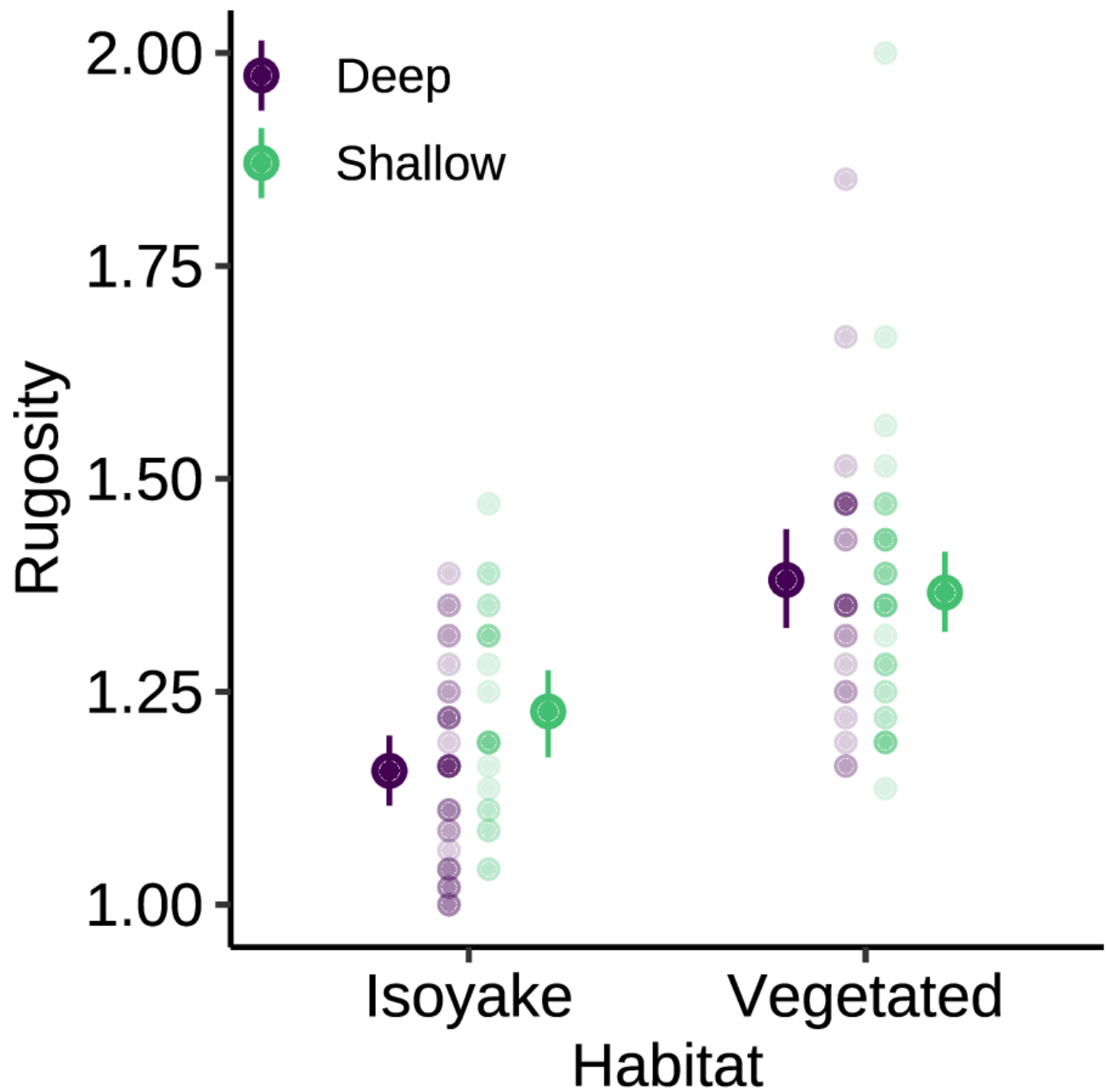
Figure 4

The results of the benthic quadrat monitoring activity.

The benthic monitoring study showing the, (A) percent benthic cover, (B) sea urchin density, and (C) sea urchin biomass from the deep and shallow transects of the isoyake and vegetated habitats. The points are the monthly observations, the solid, dashed, and dotted lines are the expectations of the generalized additive models and the shaded regions indicate the 95% highest density credible interval.
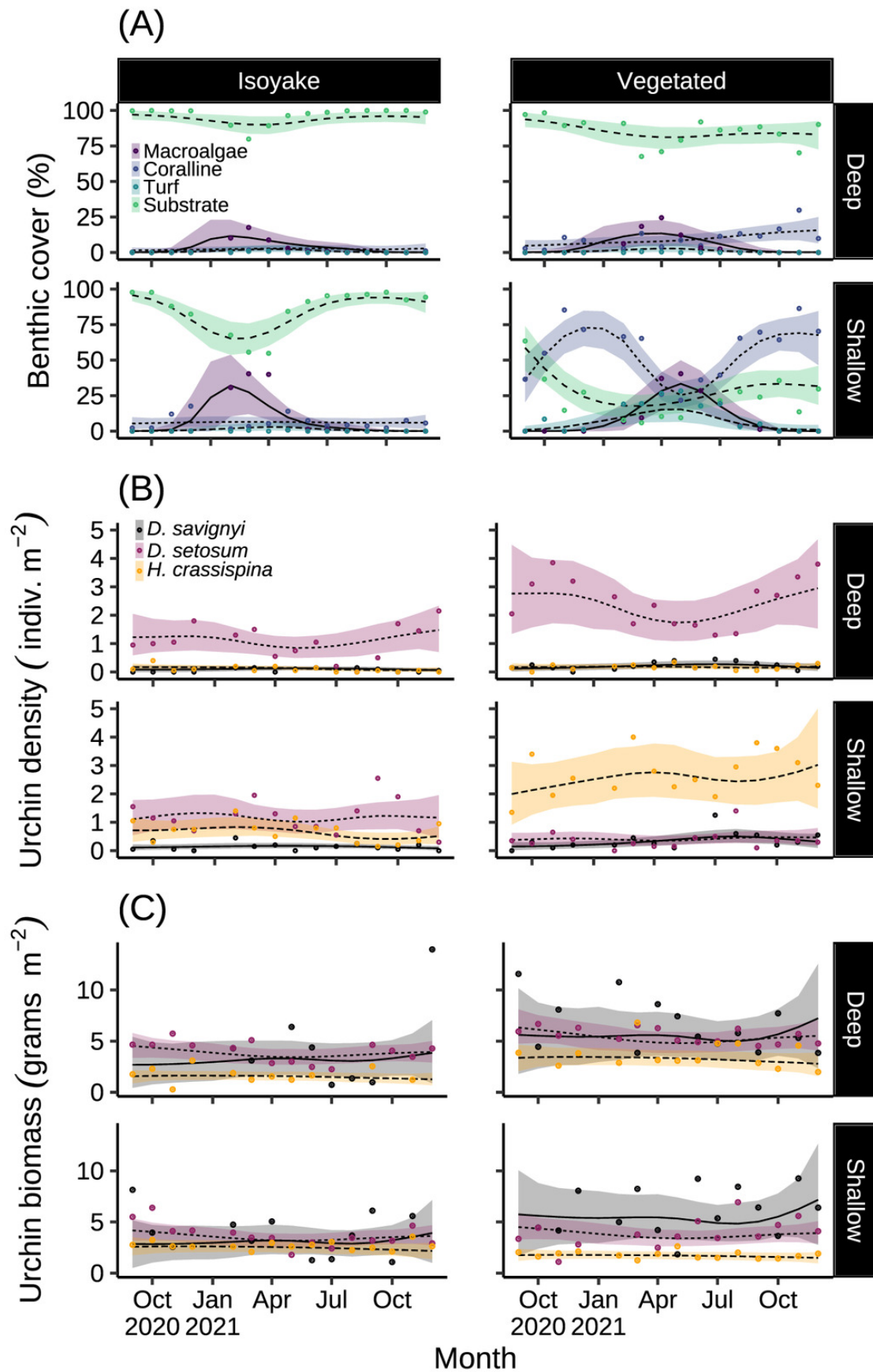
Figure 5

Quadrat photos from the isoyake habitat (IH) and vegetated habitats (VH) in seasons with (A) high and (B) low algal cover.

Quadrat photos showing the peak algal cover for (A1) deep IH and (A2) shallow IH in February and in the months of April and May for (A3) deep VH and (A4) shallow VH, respectively. The same quadrats during the low macroalgal algal cover period (< 1%) occurring in August for (B2) shallow IH and (B3) deep VH and in September for (B1) deep IH and (B4) shallow VH.
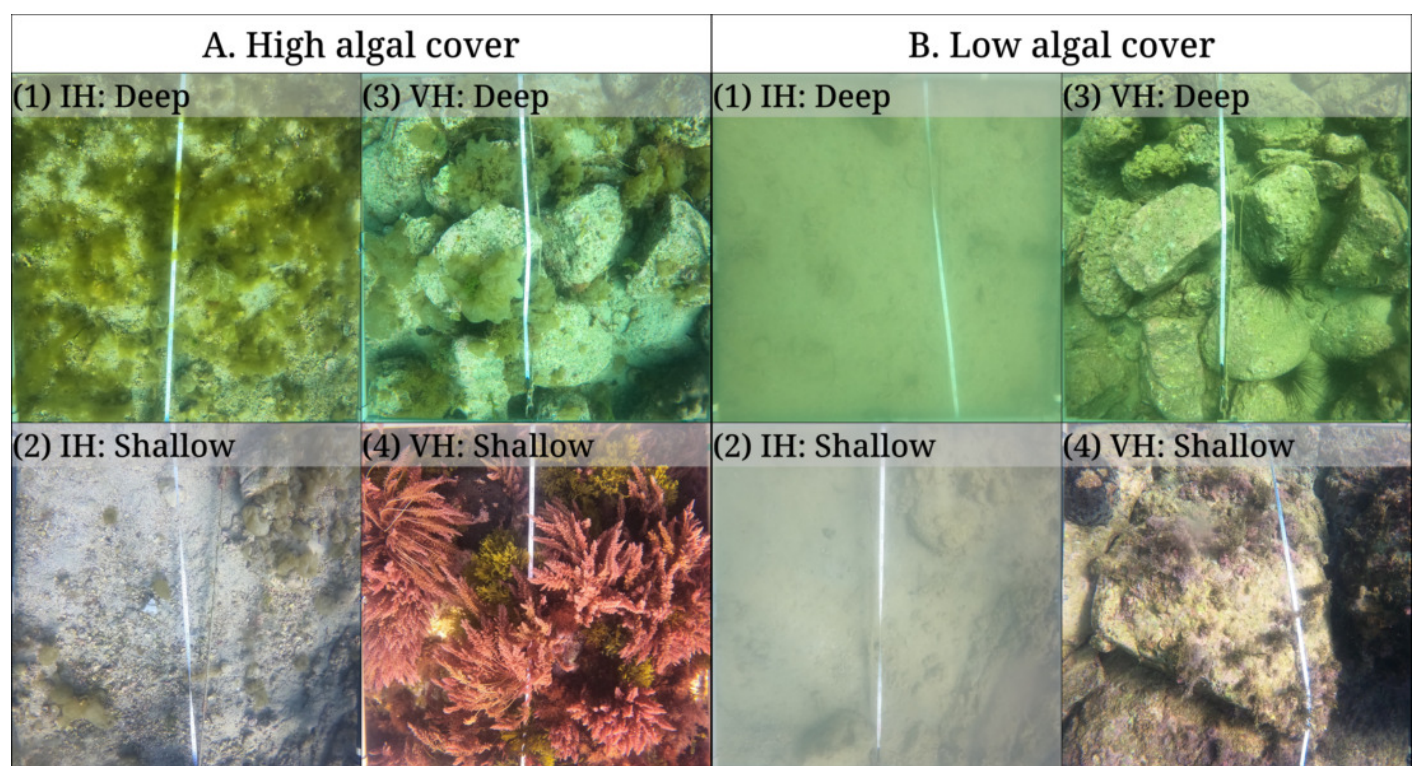
Figure 6

Sea urchin size-classes and their microhabitat preference in the (A) deep and (B) shallow isoyake habitats and the (C) deep and (D) shallow vegetated habitats.

The columns show the sea urchin species and the rows show the microhabitat type. The points are the observations, the solid, dashed and dotted lines are the expected sea urchin occurrence rate of the generalized additive model and the shaded regions indicate the 95% highest density credible interval.
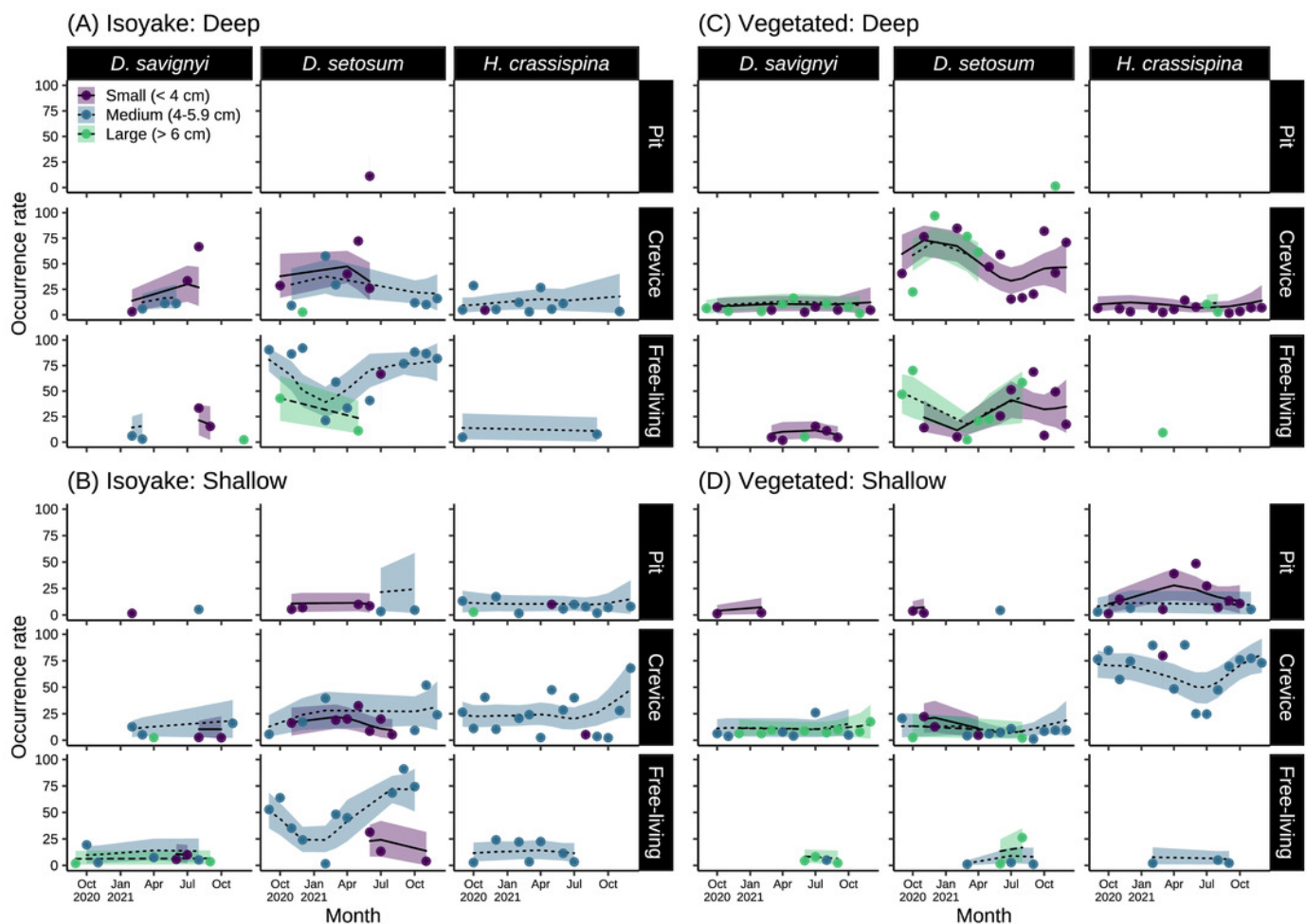
Figure 7

The results of the sea urchin mark-recapture experiment.

(A) shows the average linear displacement by the tagged *Diadema setosum* and *Heliocidaris crassispina* across the first and second recapture activity, while (B) is the change in the *D. setosum* group composition together with the tagged individuals. All tagged *H. crassispina* were solitary throughout mark-recapture experiment and were excluded from the group composition analysis. The pale-colored points indicate the observations while the solid points are the mean expected values of the generalized linear model. The vertical lines indicate the 95% highest density credible interval.
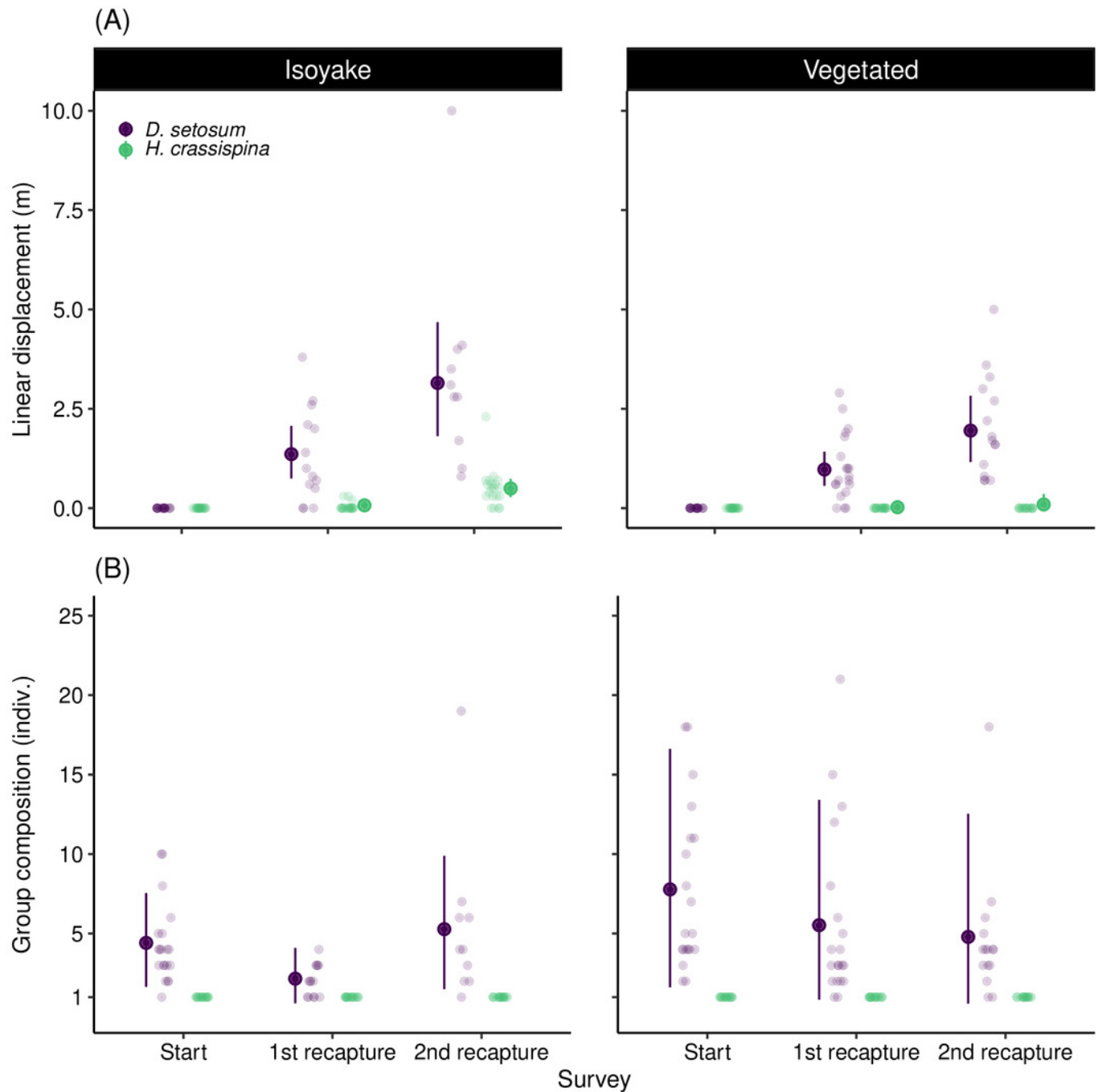
Figure 8

Sea urchin densities (indiv. m^{-2}) that describe a discontinuous phase shift.

Sea urchin densities have important thresholds that indicate the likelihood of a phase shift (see, Ishikawa et al., 2016; Kriegisch et al., 2016; Ishikawa and Kurashima, 2020). The red dotted line indicates sea urchin densities that cause a phase shift (about 8 indiv. m^{-2}). The orange dotted line indicates sea urchin densities that maintain the barren state (about 4 indiv. m^{-2}). The green dotted line indicates sea urchin densities that allow the recovery of seaweed beds (2 indiv. m^{-2} or less).
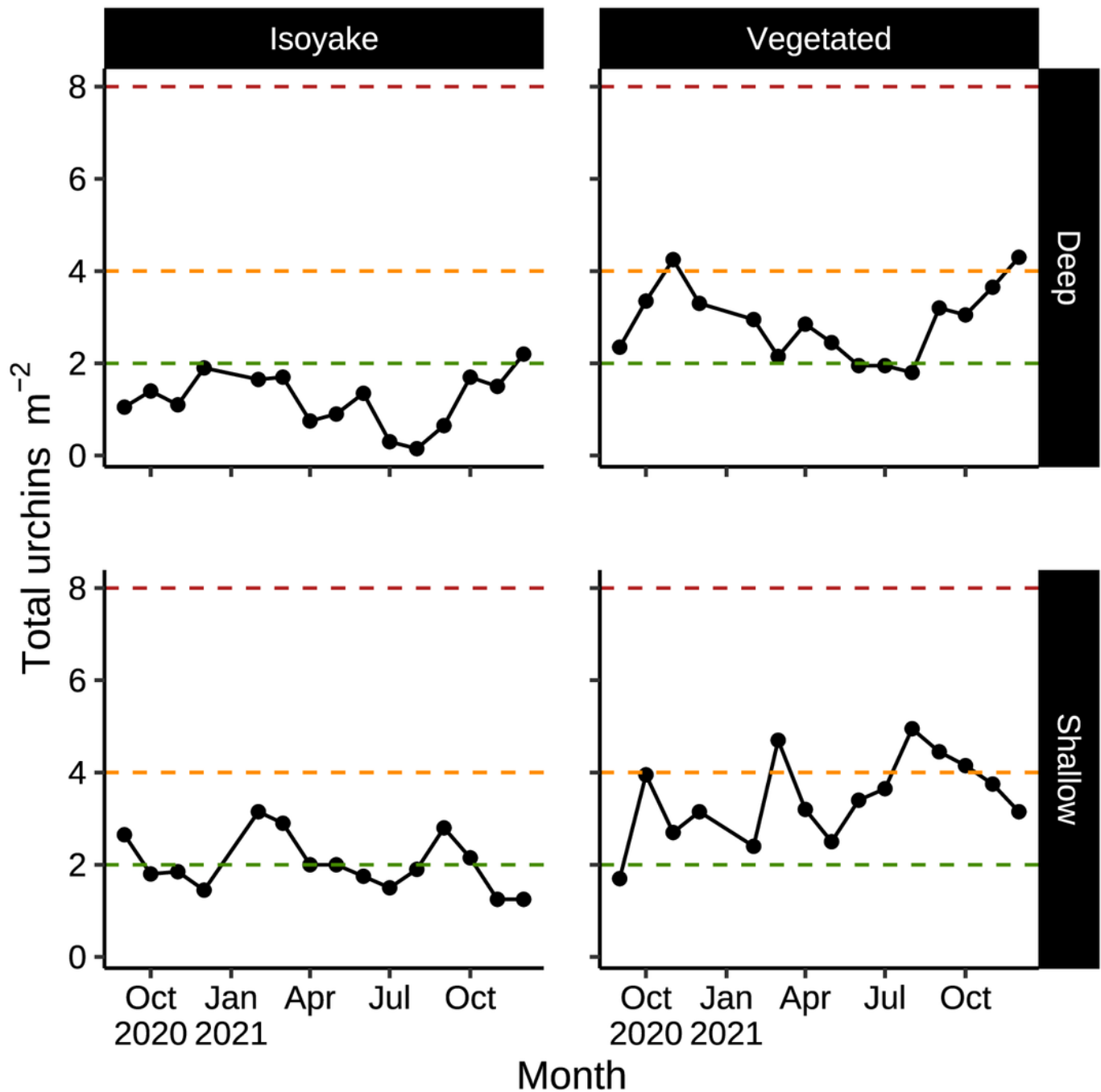
Figure 9

Comparison of the study site pre- and post-coastal development.

Maps showing the coastline of the study site, (A) before coastal armoring in the early 1970's and (B) present-day. The red dots are probable seaweed habitats that were potentially affected during the construction of the concrete jetty. Image credit: The Geospatial Information Authority of Japan (https://www.gsi.go.jp/johofukyu/johofukyu210322.html).
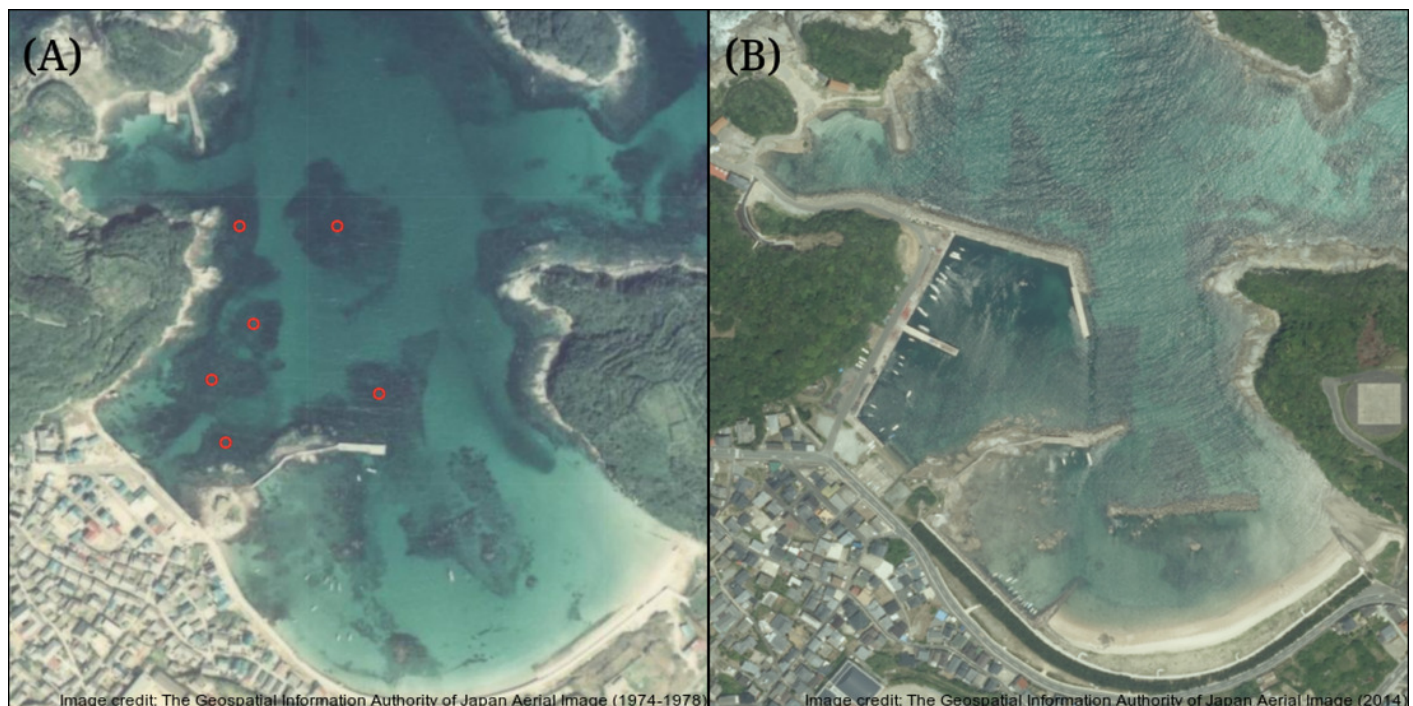
Figure 10

The annual average winter temperatures (i.e., Dec, Jan, Feb) in the vegetated habitat of Arikawa Bay since 2018.

The points are the mean values while the vertical bars are the standard deviation.
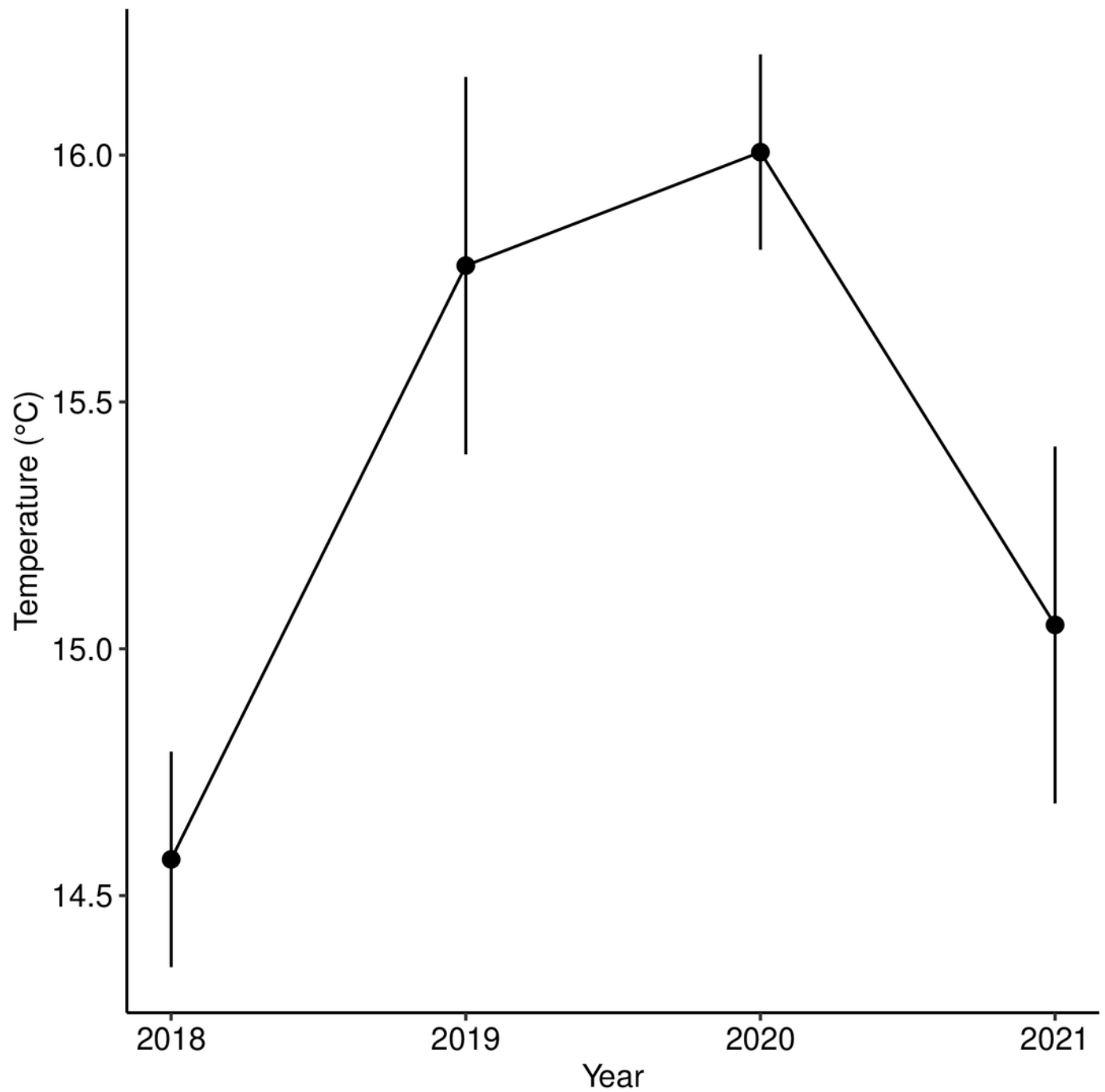
Model comparison between all models and their equivalent null model.

The values are the absolute difference in the expected log point-wise predictive density (ELPD) of the leave-one-out cross-validation (LOO) between all models and their equivalent null model. The results indicate support for the full model over the null.

Model	ELPD difference	Standard error
(A) Environmental condition models		
Wave height GAM	31.98	4.88
Light (PPFD) GAM	17.96	6.66
Temperature GAM	105.15	6.02
(B) Benthic terrain model		
Rugosity GLM	22.86	5.30
(C) Benthic cover models		
Coralline GAM	52.82	5.86
Macroalgal GAM	41.28	4.44
Substrate GAM	57.95	5.46
Turf GAM	18.57	4.91
(D) Sea urchin density models		
D. savignyi density GAM	7.31	4.99
D. setosum density GAM	20.06	7.64
H. crassispina density GAM	46.83	6.24
(E) Sea urchin biomass models		
D. savignyi biomass GAM	1.96	4.10
D. setosum biomass GAM	4.14	4.75
H. crassispina biomass GAM	14.04	6.08
(F) Microhabitat preference model		
Microhabitat GAM	88.47	13.32
(G) Sea urchin tagging models		
Linear displacement GLM	73.57	8.20
Group-size GLM	19.37	5.98

The sea urchin recapture rate and loss rate from the mark-recapture experiment conducted at the isoyake habitat (IH) and vegetated habitat (VH).

The mark-recapture experiment involved tagging *Diadema setosum* (IH: 20 indiv., VH: 20 indiv.) and *Heliocidaris crassispina* (IH: 20 indiv., VH: 20 indiv.). The species *H. crassispina* had higher recapture rates because it was less mobile while *D. setosum* had a higher loss rate, due to its higher mobility

Habitat	Species	Survey	N	Recapture rate (%)	Loss rate (%)
isoyake	*D. setosum*	start	20	100	0
isoyake	*D. setosum*	1st recapture	14	70	30
isoyake	*D. setosum*	2nd recapture	10	50	50
isoyake	*H. crassispina*	start	20	100	0
isoyake	*H. crassispina*	1st recapture	20	100	0
isoyake	*H. crassispina*	2nd recapture	20	100	0
vegetated	*D. setosum*	start	20	100	0
vegetated	*D. setosum*	1st recapture	20	100	0
vegetated	*D. setosum*	2nd recapture	15	75	25
vegetated	*H. crassispina*	start	20	100	0
vegetated	*H. crassispina*	1st recapture	20	100	0
vegetated	*H. crassispina*	2nd recapture	18	90	10